Journal of
Medicinal Chemistry

Article

Tailoring the Physicochemical Properties of Antimicrobial Peptides onto Thiazole-based #-Peptide Foldamer

Clément Bonnel, Baptiste Legrand, Matthieu Simon, Margaux Clavié, Agnès Masnou, Estelle Jumas-Bilak, Young Kee Kang, Paricia Licznar-Fajardo, Ludovic T. Maillard, and MASURIER Nicolas

J. Med. Chem., **Just Accepted Manuscript** • DOI: 10.1021/acs.jmedchem.0c00077 • Publication Date (Web): 13 Aug 2020

Just Accepted

is published by the American Chemical Society. 1155 Sixteenth Street N.W., Washington, DC 20036

Tailoring the Physicochemical Properties of Antimicrobial Peptides onto Thiazole-based γ-Peptide Foldamer

Clément Bonnel,[a]‡† Baptiste Legrand,[a] Matthieu Simon,[a] Margaux Clavié,[a] Agnès Masnou,[b] Estelle Jumas Bilak,[b] Young Kee Kang,[c] Patricia Licznar-Fajardo,* [b] Ludovic T. Maillard,*[a] Nicolas Masurier

[a] Institut des Biomolécules Max Mousseron, UMR 5247, CNRS, UM, ENSCM, UFR des Sciences Pharmaceutiques et Biologiques, 15 Avenue Charles Flahault, 34093 Montpellier Cedex 5, France.

[b] Laboratoire HydroSciences Montpellier, UMR 5569, CNRS, UM, IRD, Département d'Hygiène Hospitalière – CHU Montpellier, France.

[c] Department of Chemistry, Chungbuk National University, Cheongju, Chungbuk 28644, Republic of Korea.

KEYWORDS: Antimicrobial peptide, foldamer, thiazole-based γ-peptide.

ABSTRACT: Antimicrobial peptides (AMPs) are amphipathic molecules displaying broad-spectrum bactericidal activity providing opportunities to develop new generation of antibiotics. However their use is limited either by poor metabolic stability or high hemolytic activity. We herein addressed the potential of thiazole-based γ-peptide oligomers named ATCs as tunable scaffolds to design poly-cationic AMPs mimetics. Knowing the side chain distribution along the backbone, we rationally designed facially amphiphilic sequences with bactericidal effect in the micromolar range. Since no hemolytic activity was detected up to 100 μM, this class of compounds has shown the potential for therapeutic development.

INTRODUCTION

The rapid expansion of drug-resistant infections is a public health issue of paramount importance. In this race for effective treatments that circumvent bacterial resistance, antimicrobial peptides (AMPs) provide opportunities to develop new generation of antibiotics as they display a broad-spectrum bactericidal activity.[1-8] AMPs are typically 12 to 80 residues in length and span several secondary structures including β-sheet, α-helix, extended conformation

and loop. Most are poly-cationic sequences with a spatial segregation of the cationic and hydrophobic side chains onto distinct regions or faces of the molecule. These features are crucial to initiate electrostatic interactions with the negatively charged components of the bacterial envelope[9] and to insert into the phospholipid bilayer leading to depolarization or disruption of the bacterial cell wall.[10] Although other mechanisms of action have been proposed,[11] it is widely believed that such a simple physicochemical destabilization of the membrane results in a relatively low propensity to elicit bacterial resistance.[12, 13] However, due to poor metabolic stability and frequent hemolytic activity, most AMPs have faced some difficulties for practical clinical applications.[2, 14]

To overcome these issues, one has proposed to tailor the physicochemical characteristics of AMPs onto new classes of non-natural polymers.[15] Peptidomimetic antimicrobials have first been made using folded amphipathic β-peptides.[16-21] Beside a broad-spectrum bactericidal activity, they offer the additional advantage of being resistant to proteases. However, as for many AMPs,[22, 23] the first generation compounds have low discrimination for bacterial *versus* mammalian cells resulting in toxic side effects such as hemolysis.[16] Following these pioneer results, other folded architectures such as peptoids,[24]

oligo-ureas,[25, 26] arylamides[27-29] or arylureas[30-32] and phenylene ethylenes[33] have been used to template the facially amphiphilic morphology of natural AMPs. In particular, Brilacidin (PMX-30063) an arylamide foldamer has to date completed a Phase 2b clinical trial with positive results in serious skin infections,[34] demonstrating the therapeutic potential of AMPs-mimicking antibiotic agents.

Over the last years, our group described a class of constrained heterocyclic γ-amino acids built around a thiazole ring, named 4-amino(methyl)-1,3-thiazole-5-carboxylic acids or ATCs (Fig. 1a),[35] which were initially used to template an amphipathic hairpin peptide with antibacterial activities analogous to gramicidin S.[36] Furthermore, ATC containing oligomers showed high propensity to adopt defined structures in both organic solvents and water.[35, 37, 38] The facial anisotropy of the edifice enables a precise 3D positioning of the appended functionalities making ATC γ-peptides suitable for material[39] and biomedical applications.[40, 41] In line with our research agenda, we herein addressed the prospects of ATC oligomers as tunable scaffold to design poly-cationic AMPs mimetics.

RESULT AND DISCUSSION

Design of ATC-based AMPs mimetics. ATC oligomers are closed to a C_3-symmetry helix with three residues to achieve a whole turn.[35] The helical folding results from a hydrogen-bonding network of the type (*i*, *i*+2). The six substituents per turn define three distinct faces over the γ-peptide (Fig. 1b). As example, side-chains at γ-position of residues *i* and *i+3* and the one decorating the thiazole ring of residue *i+1* share the same face. On the basis of this topology, we initially designed four sequences **1**-**4** with three to twelve ATC units and +2 to +8 cationic charges, by repeating the same tripeptide pattern. While two faces distributed methyl substituents, the third one displayed cationic aminobutyl side chains (Fig. 1c). We also prepared sequence **5**, a scrambled isomer of **4** with the height cationic charges distributed all around the helix axis (See table S1 for the sequence). Because chain length and hydrophobic/hydrophilic balance were recognized as crucial parameters for both selectivity and affinity for bacteria, sequences **6**-**9** were considered. With one face sharing *i*-Bu substituents instead of methyls, the 12-mer **6** was predicted more hydrophobic than its counterparts **4**. In oligomers **7** and **8**, the weakly basic aminobutyl groups were changed by guanidinopropyls. Finally, in a last variation **9** the overall charge was decreased to +4 while a twelve ATCs length was preserved.

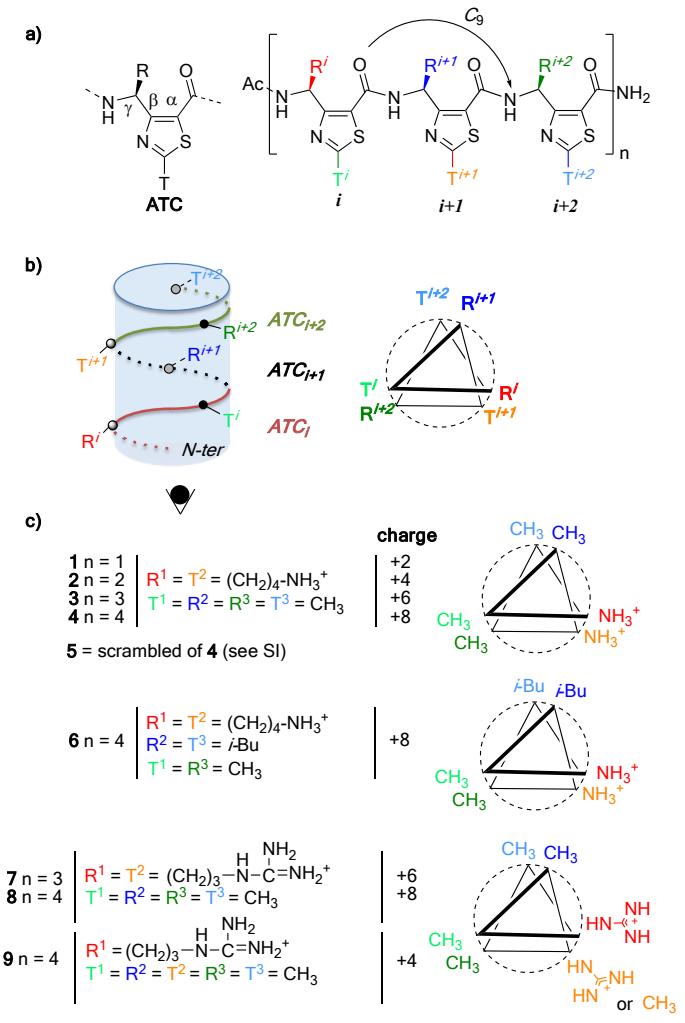

Figure 1. a) Nomenclature, typical H-bonding pattern and schematic view of the position of the side chains looking down the ATC oligomers (from *N*-terminus to *C*-terminus). b) Helical wheel diagram of canonical ATC γ-peptides. c) Designed antimicrobial γ-peptides **1-9**.

Syntheses of ATC oligomers. The general route to the *N*-Fmoc-ATC-OH monomer units **13** is reported Scheme 1. They were synthesized from the commercially available *N*-Fmoc-Ala-OH and *N*-Fmoc-Lys(Boc)-OH following

our previously reported methodology.[42] The *N*-Fmoc-amino acids were first engaged in a cross-Claisen condensation to lead the β-ketoesters whose bromination of the malonic position was done with NBS and a catalytic amount of $Mg(ClO_4)_2$. The subsequent α-bromo-β-ketoesters **11** were then reacted with the appropriate thioamides depending on the required side chain at position 2 of the thiazole ring. Finally, chemoselective deprotection of the dimethylallyl esters was carried out under Tsuji-Trust conditions to yield the *N*-Fmoc-ATC-OH **13**. *N*-Fmoc-ATC-OH **13a-d** were previously described.[42] The *N*-Fmoc-ATC-OH building-blocks **13e-h** were prepared as reported in Scheme 2. Isothiovaleramide was synthesized in two steps starting from isovaleryl chloride in 43% overall yield. Hantzsch cyclization with **11a** led to the fully protected ATC **12e** (41%). *N*-Boc-5-aminovaleric **14** was reacted with *i*-butylchloroformate and gaseous ammonia to quantitatively yield *N*-Boc-5-aminovaleramide **15**, which was converted to the corresponding thioamide with Lawesson reagent (50%). A two steps cyclization with either the α-bromo-β-ketoester **11a** or **11b** and deprotection of the dimethylallyl ester led to *N*-Fmoc-ATC-OH **13f-g**. Finally Boc-GABA-OH **19** was considered for the synthesis of the monomer unit **13h** that displayed a di-Boc-Guanidinopropyl side chain. After conversion of Boc-

GABA-OH into the corresponding thioamide **21**, the Boc group was removed under acidic conditions. The resulting free amine was reacted with the 1,3-Di-Boc-2-(trifluoromethylsulfonyl) guanidine **25** to yield the thioamide **26**, which was then condensed in basic conditions with the α-bromo-β-ketoesters **11a**. Aromatization of the hydroxythiazoline was obtained by treatment with trifluoroacetic anhydride (TFAA) DIEA. The *N*-Fmoc-ATC-OH **13h** was finally obtained after deprotection of the dimethylallylester under Tsuji Trost conditions.

Scheme 1. Synthesis of *N*-Fmoc-ATC-OH and γ-peptides 1-9.

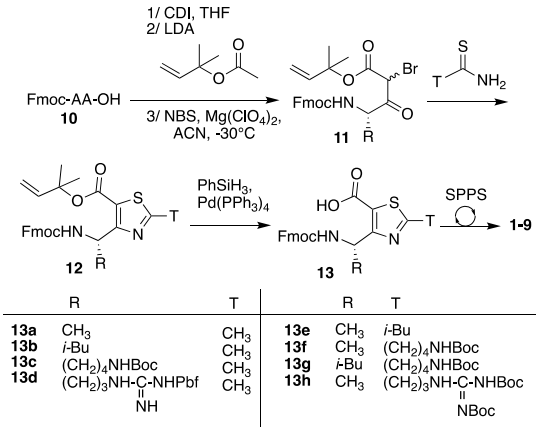

	R	T		R	T
13a	CH_3	CH_3	**13e**	CH_3	*i*-Bu
13b	*i*-Bu	CH_3	**13f**	CH_3	$(CH_2)_4NHBoc$
13c	$(CH_2)_4NHBoc$	CH_3	**13g**	*i*-Bu	$(CH_2)_4NHBoc$
13d	$(CH_2)_3NH$-C(=NH)-NHPbf	CH_3	**13h**	CH_3	$(CH_2)_3NH$-C(=NBoc)-NHBoc

Stepwise elongations of peptides **1-9** were done on Rink amide resin following a Fmoc/*t*-Bu SPPS strategy. Couplings were performed at r.t. over night using DIC/Oxyma Pure as reagent and NMM as base. It was found that decreasing the time reaction or changing the coupling reagent led to incomplete reactions. The

N-termini were capped with Ac_2O then cleavages from the solid support and deprotections of the aminobutyl side chains were performed by TFA/TIS/H_2O (95/2.5/2.5). All the sequences were finally purified by reverse-phase HPLC.

Scheme 2. Chemical route to *N*-Fmoc-ATC-OH 13e-h.

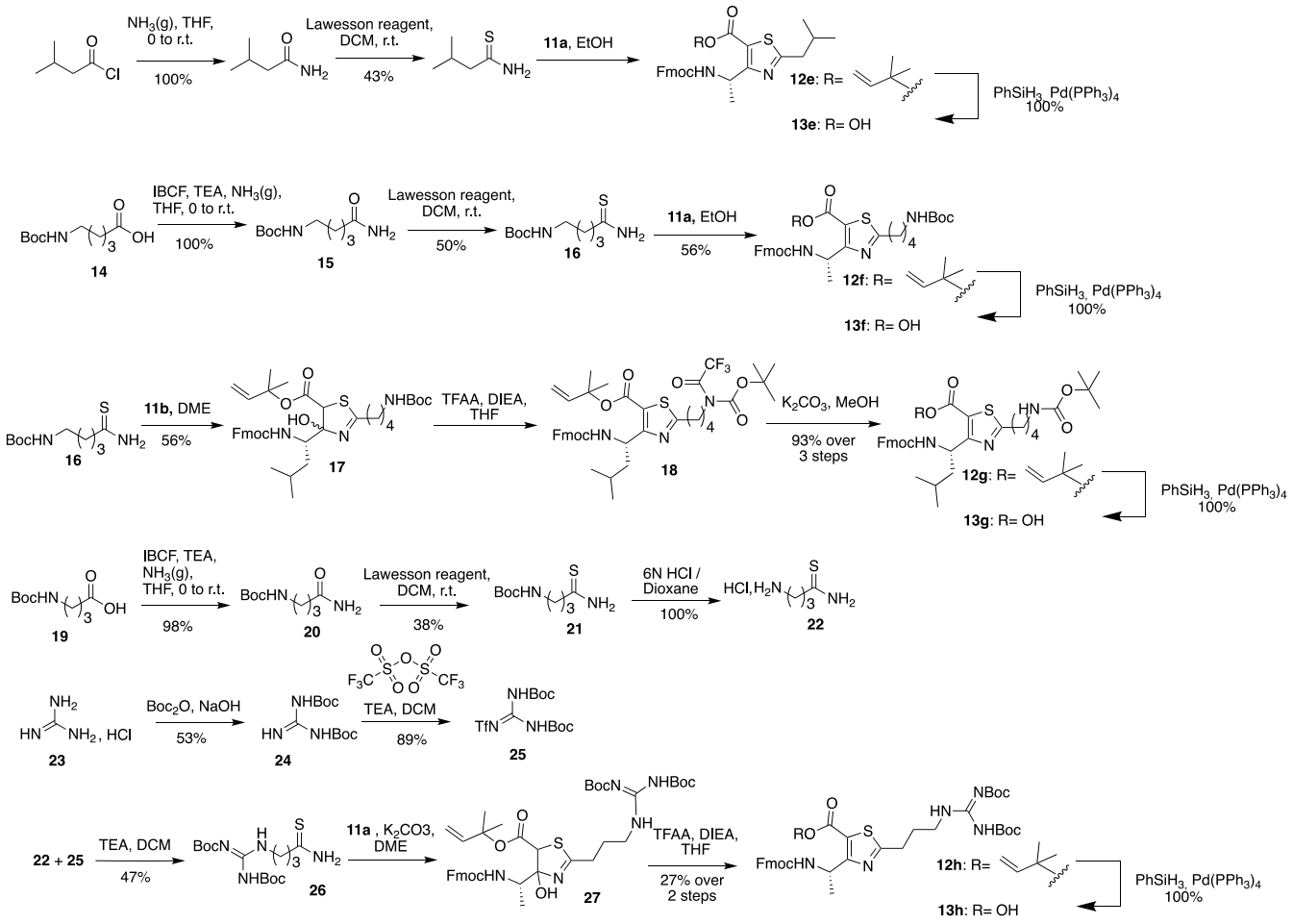

Circular dichroism. The folding behaviors of oligomers were first assessed by CD in water (pH 6.0) at 25 μM between 200 and 300 nm. Irrespective of the peptide, the CD signatures displayed two negative minima at 208 and 220 nm and a strong positive maximum at 265 nm, which is consistent with a C_9-helical

folding.[35] In addition, the molar ellipticity values per residue (73600 deg.cm^{-2} dmol^{-1} at 265 nm) were similar to the previously reported value (74000 deg.cm^{-2}.dmol^{-1}) reported for helical ATC-oligomers in water.

FT-IR studies. We showed in a recent study that the amide I frequencies provide unambiguous structural indicators of the H-bond network for helically folded ATC-containing oligomers.[37] Free ATC carbonyls were expected to give amide I absorption at ν(CO)>1640 cm^{-1} (1645 cm^{-1} for ATC-CONH-R and around 1675 cm^{-1} for ATC-CONH$_2$) while the bounded ATC C=O should be highly redshifted around 1620-1625 cm^{-1}. Fig. 2B shows the spectrum of oligomer **3**, which is representative of the entire series (Fig S3 and Table S13). The band at 1618 cm^{-1} was attributed to the bound ATC C=O. No band was observed around 1645 cm^{-1}, which confirmed that most of the ATC carbonyls were involved in hydrogen-bonds as expected for a C_9-helical folding. Because oligomers were obtained as trifluoroacetate salts, strong absorption bands at 1147 cm^{-1} and 1198 cm^{-1} corresponding to C-F stretching modes were also observed. The band at 1678 cm^{-1} was attributed to the overlay of carbonyl vibrations corresponding to the trifluoroacetate salts and to the C-terminus ATC-CONH$_2$. Estimations of contributions of discrete subcomponent absorptions in the amide I region have

been achieved using curve-fitting approaches with Gaussian functions. Quantitative analysis revealed that the absorption at 1619 cm^{-1} and 1678 cm^{-1} contributes to 55% and 45% of the C=O components respectively that perfectly settled the C_9-helical structure (eleven bound ATC C=O *vs* one free ATC C=O and six TFA).

NMR analyses and structure calculation: We finally explored the folding of the oligomers by NMR. NMR analyses of **3** and **4** were conducted in H_2O/D_2O (9:1), pH 6.5. In the case of oligomers **6-9**, NMR analysis could not be conducted in water because of poor ^1H signal dispersion but nearly all backbone resonances of **6-9** could be assigned in CD_3OH. As previously observed on ATCs-containing oligomers,[35, 36] all the amide protons signals were strongly downfield. Such a strong NH deshielding (> 9 ppm) has been recognized as a structural marker related to the formation of the C_9 hydrogen-bonding pattern.[37] In addition, $^3J(NH,^{\gamma}CH)$ values < 6 Hz (5.3 ± 0.3 Hz) were typical of ϕ values around -60° (Table S8) as expected for a C_9-helix. Further evidences of C_9-helical folding came from the analysis of the 2D-ROESY spectra, which revealed characteristic medium sequential NH(*i*)/$^{\gamma}$CH(*i*-1) and weak $^{\gamma}$CH(*i*-1)/$^{\gamma}$CH(*i*) correlations. In the case of oligomer **3**, many weak NH(*i*)/$^{\delta}$CH(*i*-1), NH(*i*)/$^{\varepsilon}$CH(*i*-1) and $^{\gamma}$CH(*i*-

1)/$^{\delta}$CH(i) NOE connectivities documented as structural markers of the ATC helix were visible (Fig. 2C and Tables S8).[37] For the longer sequence **4**, and for oligomers **6**-**9** these canonic weak NOEs were also detectable but could not be unequivocally assigned due to signal overlaps.

Taking all together, the NMR, FT-IR and CD data were strong evidences of the facially amphiphilic morphology of the designed γ-peptides. NOEs were finally used as restraints for NMR solution structure calculations of **3** using a simulated annealing protocol with AMBER 16.[43] Unambiguous 99 distance restraints were introduced to generate an ensemble of convergent 15-lowest energy structures in water (Fig. 2D). The lowest energy structure has been further optimized with Gaussian 09[44] at the SMD M06-2X/6-31G(d) level of theory in water and its electrostatic potential was calculated at the same level of theory (Supporting Information). As expected, we obtained a well-defined C_9-helix in which all the cationic lateral chains were distributed along a single face (Fig. 2E, Table S12). By contrast to the majority of cationic AMPs, which are intrinsically disordered in solution because of electrostatic repulsion between the side chains, oligomer **3** was folded. The length of the oligomer is 34.7 Å with three helical turns, each displaying a pitch of 11.5 Å as previously reported.[35]

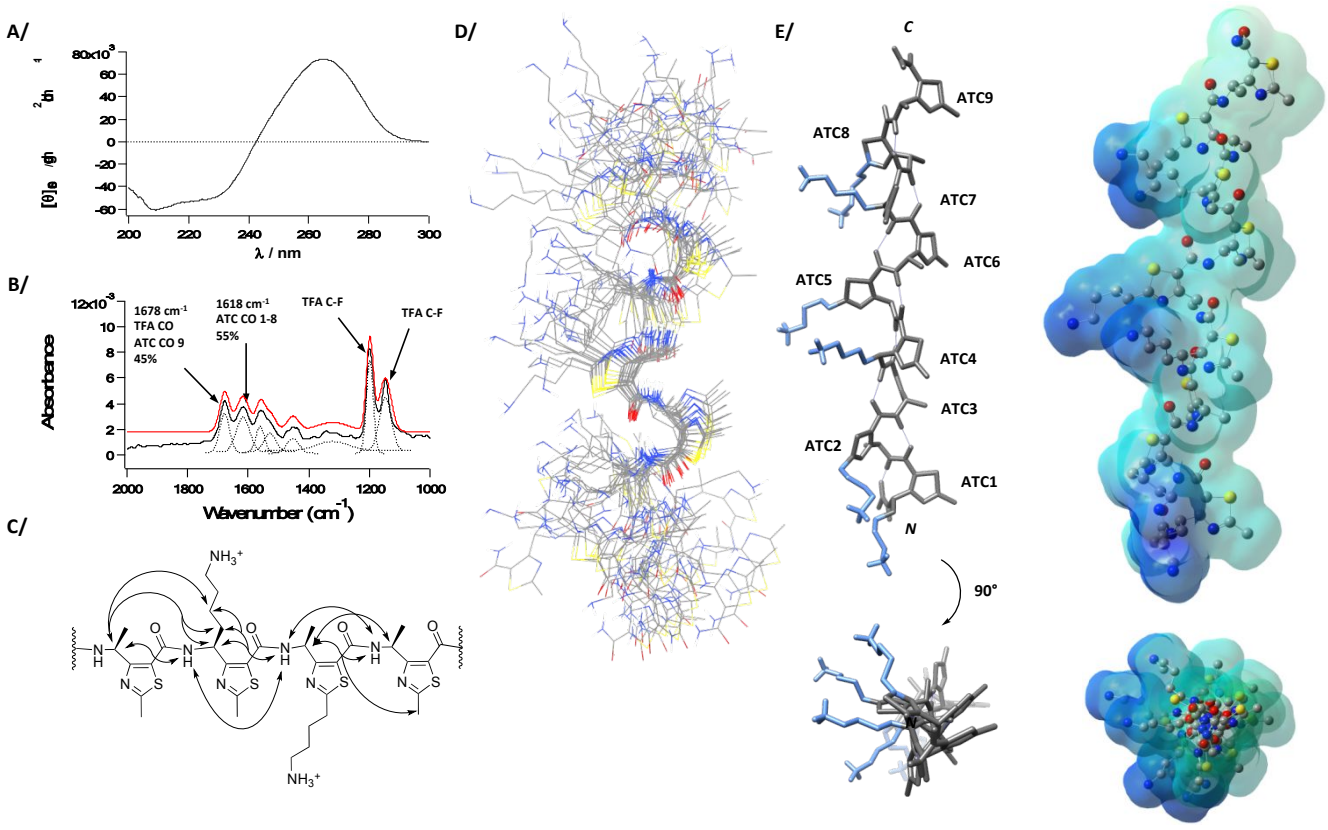

Figure 2. A/ Far-UV CD spectrum of **3** in water (pH 4.3) at 25 μM between 200 and 300 nm. B/ FT-IR spectrum (Black) and deconvolution (Red) of oligomer **3** in the Amide I in water (pH 4.3) at 5 mM. C/ Typical Inter-residue NOEs pattern along **3** in water pH 6.5. D/ Superimposition of the 15 lowest energy NMR solution structures of the oligomer **3** in water. E/ Lowest-energy NMR structure of compound **3** optimized at the M06-2X/6-31G(d) level of theory in water using the solvation model based on density (SMD) method and its electrostatic potential (color scale: blue +0.541e, green 0e, red -0.541e) calculated using the Merz-Singh-Kollman scheme at the same level of theory in water.

Relative hydrophobicity of 3-9. Since the hydrophobic/hydrophilic balance is recognized as a crucial parameter influencing both selectivity and affinity for bacteria, we examined the relative lipophilicity of the oligomers by RP-HPLC. The percentage of acetonitrile required for elution of peptide **3-9** from C18 analytical column are listed Table S14. Variations in elution properties of sequences **3**, **4**, **7** and **8** were small indicating very similar lipophilic properties. However, as expected for molecules displaying a much larger hydrophobic surface resulting from branched lateral chains, HPLC analyses showed that oligomer **6** was more lipophilic than all the other sequences. Reducing the overall charge as in compound **9** also led to a similar polarity decrease. Nevertheless, all the peptides remained highly soluble in water (up to 10 mM, pH 4.0 to 7.5).

Antimicrobial activity. Minimal inhibitory concentration (MIC) and Minimal bactericidal concentration (MBC) values (Table 1) were determined against both Gram-positive (*Bacillus subtilis*, *Staphylococcus aureus, Enterococcus faecalis*) and Gram negative (*Escherichia coli, Pseudomonas aeruginosa*) bacteria as well as a yeast

(*Candida albicans*). Three independent experiments were conducted using Melittin, the main cytolytic component of the bee venom, as positive control. Comparison of oligomers **1**-**4** shows a strong correlation between sequence length and activity. While shorter oligomers **1** and **2** were little to no active, 9-mer **3** showed significant bactericidal activity, which is even more marked with the longest peptide **4**. Since the sequences **3** and **4** span a length of 34.7 Å and 46.3 Å that match the membrane thickness ~35-40 Å, it is likely that antimicrobial activity results from perpendicular insertion of peptides into the lipid bilayer as proposed in the barrel-stave and toroidal models.[45, 46] The scrambled **5** peptide remained active on *B. subtilis* which is the most sensitive strain regardless of the compound. However it was three to almost twenty-five times less potent on the other bacteria than the facing sequence **4** demonstrating that controlling spatial segregation of the cationic chains is important for the antimicrobial effect. Based on results obtained with **1**-**4**, sequence lengths of **6**-**9** were fixed at nine and twelve monomer units. As shown in Table 1, the 12-mer **8** displaying guanidine groups was the most potent among the all series and compared to its parent **4,** showed an antimicrobial spectrum extended toward *S. aureus* and *E. faecalis*. Reducing the overall charge (compound **9**) increased the

selectivity toward Gram + bacteria while decreasing the activity on Gram - germs and *C. albicans*.

Table 1. Antimicrobial and hemolytic activities of ATC-containing oligomers 1-9

			Gram +			**Gram -**		**Yeast**	
Sequence	**Length (n=)**	**Charge**	*B. subtilis* ATCC6633[a]	*S. aureus* ATCC6538[a]	*E. faecalis* ATCC29121[a]	*E. coli* ATCC8739[a]	*P. aeruginosa* ATCC9027[a]	*C. albicans* ATCC10231[a]	**HD_{50}[b]**
Melittin			0.8 (1.1)	0.9 (1.2)	1.6 (1.6)	3.4 (4.7)	3.1 (3.1)	1.6 (1.6)	3
1	1	+2	>150 (>150)	>150 (>150)	>150 (>150)	>150 (>150)	>150 (>150)	>150 (>150)	> 100
2	2	+4	30 (30)	>150 (>150)	>150 (>150)	>150 (>150)	>150 (>150)	62.5 (130)	> 100
3	3	+6	0.8 (0.8)	>150 (>150)	>150 (>150)	5.2 (7.3)	42 (83)	10.4 (10.4)	> 100
4	4	+8	0.5 (0.5)	26 (57)	>150 (>150)	1.6 (1.6)	3.9 (5.2)	3.7 (3.7)	> 100
5	4	+8	0.8 (0.8)	100 (>100)	>150 (>150)	5.2 (8.3)	100 (>100)	50 (62.5)	> 100
6	4	+8	4.2 (6.2)	16.7 (25)	10.4 (12.5)	14.6 (16.5)	14.6 (19)	25 (25)	>100
7	3	+6	0.5 (0.5)	14.6 (16.5)	100 (>100)	0.8 (0.8)	54 (100)	9.4 (12.5)	>100
8	4	+8	0.6 (0.8)	3.1 (7.8)	20.8 (25)	1.8 (2.3)	4.2 (4.7)	6.2 (6.2)	>100
9	4	+4	0.5 (0.5)	3.1 (8.3)	3.1 (11.5)	23 (30)	> 100 (nd)	25 (50)	46

[a] Minimal inhibitory concentration (MIC) values in μM for ATC-peptides 1-9. Minimal bactericidal concentration (MBCs) values in μM are indicated in bracket [b] dose required to lyse 50% of the red blood cells (HD_{50}) are in μM. nd not determined

Hemolytic activities. We next investigated the susceptibility of human cells to oligomers **3**-**9** by monitoring erythrocytes lysis. Interestingly, no hemotoxicity was detected up to 100 μM for most of the γ-peptides, including the most active one **8**, compared to melittin (HD_{50}=3 μM). Only the 12-mer **9** with an overall

charge of +4 led to significant hemolysis. This result is consistent with other reports demonstrating correlations between hydrophobicity and bacteria cell selectivity.[19, 47]

SEM experiments: Based on these results, we chose to focus on the most potent oligomer **8** and evaluated its impact on *E. coli* morphology by surface electron microscopy (SEM). In order to define the best incubation period to observed antimicrobial effects, we conducted time-kill study on *E. coli* over 2h incubation at 37°C. The average log reduction of the viable cell count ranged between 0.95 and 4.73 $\log_{10}$ cfu/ml on incubating the bacteria for 2 h at the MIC and 8xMIC. Significant decrease of the growth rate was observed between 40 to 60 min at 4x and 8xMIC (Fig. S4). Once again such a fast killing kinetic is consistent with a mechanism involving membrane destabilization. Thus we decided to perform TEM experiments after 60 min contact between bacteria cells and compound **8**. The untreated *E. coli* cells were about 2.0 μm long and displayed a smooth and intact surface (Fig. 4A-B). After incubation with peptide **8**, the bacteria shortened to as little as 1.3 μm and appeared more compact indicating that the bacteria were not able to grow to maximum length (Fig. 4C-E). As previously observed with other helical AMPs,[48] the cells exhibited increased region of cellular

aggregation. Beside these changes of morphology, the cells showed blisters and protruding vesicles on their surface (Figure 3E). In addition, whereas there were no fragments for control untreated bacteria, numerous spherical elements whose diameters were lower than 0.1µm were observed around bacteria, the number of which increasing with the peptide concentration. Despite some dispersion in size, such fragments, probable microsomes, were classically reported with other AMPs associated with membrane permeation and/or depolarization.[48-50] Finally, at supra-MIC numerous lysed cells were observed.

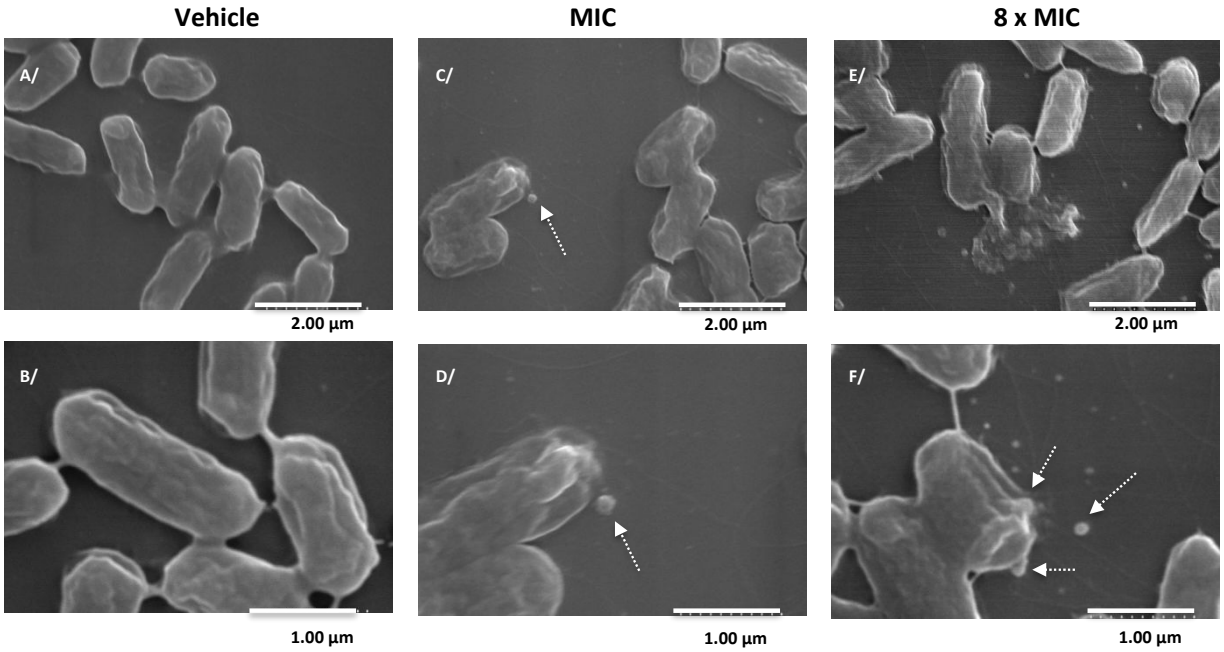

Figure 4. A/, B/ SEM micrographs untreated *E. coli* on glass platelets. In isotonic medium the cells are long, intact and evenly shaped. C/ and D/ After 60 min incubation

with MIC of **8**, the cells appear shorter and more compact and showed protruding vesicles on their corrugated surface. E/ and F/ After 60 min incubation with 8xMIC of **8**, blisters were visible on cell surface leading to numerous spherical elements in the medium and numerous lysed cells were observed.

Mechanistic studies: To get more evidences of the mode-of-action of **8**, we performed membrane depolarization experiments on *E. coli*. The modifications in ion permeability was studied using 3,3′-Dipropylthiadicarbocyanine iodide [*DiSC3*(*5*)], a voltage-sensitive fluorescent probe. The carbocyanine accumulates on polarized membranes resulting in self-quenching of fluorescence while upon membrane depolarization, the dye is released and fluorescence de-quenched.[51-53] Melittin was chosen as a positive control and cefotaxim and ampicillin as negative control. As expected for membrane-active antimicrobial peptides, both melittin and compound **8** cause a dose-dependent increase of membrane depolarization at bactericidal concentrations (Figure S5).

Evaluation of resistance development: we finally conducted antibiotic resistance experiments. Experiments were performed to measure the susceptibility of *E. coli* to develop resistance against one conventional antibiotic, cefotaxim and melittin as well as **8**. These experiments were performed by a serial passage of *E. coli* to sub-lethal concentrations of the three compounds,

followed by determination of the MIC values every 24 h period. For cefotaxim the MIC increased in as little as five exposures, and raised from <0.05 μg/ml to 0.8 μg/ml after the 8th passage. In contrast, no significant change in the MIC was observed for **8** and melittin over the entire time course of the experiment in sharp contrast to the conventional antibiotic.

CONCLUSION

This work illustrates the potential of ATC-based γ-peptide oligomers as scaffold for the development of poly-cationic AMPs mimetics. Knowing the side chain distribution along the backbone, we rationally designed facially amphiphilic sequences with three to twelve ATC units. By contrast to the majority of cationic AMPs, which are intrinsically disordered in solution because of electrostatic repulsion between the side chains, ATC oligomers retain a well-defined secondary structure without the need for membrane binding or helix promoting organic solvents. We first explored the relationship existing between the oligomer size and the antimicrobial activities and identified that a minimum of nine residues is necessary to gain antibacterial effects. In addition, we demonstrated that a spatial segregation of the cationic and hydrophobic side chains is important for the antimicrobial effect. Among the nine peptides

described, oligomer **8** was the most potent in term of *in vitro* antimicrobial activity and cell specificity. Much important is that we didn't detect any hemolytic activity even at 100 μM, which is crucial for the development of i.v. antibiotics. While detailed mechanisms of action for **8** cannot be extracted solely from the data reported here, SEM images were consistent with membrane alteration mechanisms as expected for poly-cationic amphiphilic molecules.

EXPERIMENTAL SECTION

General procedures. All reagents and solvents were obtained from commercial sources and used without further purification. Analytical HPLC analyses were run on an Agilent Technology 1220 Infinity LC equipped with a Chromolith Speed Rod RP-C_{18} 185 Pm column (50 x 4.6 mm, 5 μm) with a gradient from 100% (H_2O/TFA 0.1%) to 100% (CH_3CN/TFA 0.1%) in 5 min; flow rate 4 mL/min; UV detection at 214 nm (conditions B). Retention times are reported as follows: Rt = (min). LC/MS analyses were recorded on a Quattro *micro*™ ESI triple quadrupole mass spectrometer (Micromass, Manchester, UK) equipped with a Chromolith Speed Rod RP-C18 185 Pm column (50 x 4.6 mm, 5 μm) and an Alliance HPLC System (Waters, Milford, USA); gradient from 100% (H_2O/HCO_2H 0.1%) to 100% (CH_3CN/HCO_2H 0.1%) in 3 min; flowrate 3 mL/min;

UV detection at 214 nm. High-Resolution Mass Spectrometric analyses were performed with a time-of-flight (TOF) mass spectrometer fitted with an Electrospray Ionisation source (ESI) in positive ion mode. Intermediates **11** and *N*-Fmoc-ATC-OH **13a-d** have been synthesized as previously reported.[42] All oligomers **1-9** tested for biological activity showed > 95% purity as assessed by RP-HPLC (Chromolith Speed Rod RP-C18 185 Pm column 50x4.6 mm, 5 μm; flow rate: 5.0 mL/min; gradients from 100/0 to 0/100 eluents A/B over 5 min, in which eluents A=H_2O / TFA 0.1% and B=CH_3CN / TFA 0.1%; Detection was done at 214 nm).

isovaleramide: Isovaleryl chloride (1.0 equiv., 16.6 mmol, 2.0 mL) was diluted with 20 mL of dry THF under an argon atmosphere. Then ammoniac was bubbled into the solution for 30 min at 0°C and the white turbid mixture was evaporated to quantitatively yield isovaleramide as a white powder which was used without further purification. ^{1}H NMR (400 MHz, DMSO-d_6) δ 0.83 (d, J = 6.4 Hz, 6H); 1.90-1.93 (m, 3H); 6.72 (s, 1H); 7.21 (s, 1H).

isothiovaleramide: Isovaleramide (1.0 equiv., 16.6 mmol) was dissolved in dimethoxyethane (DME, 120 mL) and Lawesson's reagent (0.55 equiv., 9.1 mmol, 3.7 g) was then added in one portion. The mixture was refluxed at 100°C for 2 h

(HPLC monitoring). Solvent was evaporated and the yellowish residue was dissolved in a mixture of EtOAc (100 mL) and aqueous saturated $NaHCO_3$ solution (100 mL) which was stirred for 15 min. After transfer in a separating funnel, the organic layer was washed with brine, dried over $MgSO_4$, filtered and concentrated under reduced pressure to yield crude product (yellow oil) which was purified by flash chromatography on silica gel (DCM 100% to DCM/MeOH: 94/6) to yield pure isovaleric thioamide as slight yellow crystals. Yield 43 % (841 mg). ^{1}H NMR (400 MHz, DMSO-d_6) δ 0.98 (d, J = 6.6 Hz, 6H, H_1); 2.23 (m, 1H, H_2); 2.50 (d, 2H, J = 6.9 Hz, H_3); 6.90 (br, 1H, NH_5); 7.76 (br, 1H, NH_5). LC Rt = 1.00 min. LC-MS: (ESI+): m/z 118.2 ($[M+H]^+$) 100%.

1,1-dimethylprop-2-en-1-yl 4-[(1*S*)-1-(N-Fmoc)-aminoethyl]-2-isobutyl-1,3-thiazole-5-carboxylate (12e): A solution of **11a** (1.0 equiv., 4.5 mmol, 2.25 g) and isovaleric thioamide (1.6 equiv.) in EtOH was stirred 4 h at 40°C. After evaporation of the solvent, the crude product was purified by flash chromatography (Cyclohexane 100% to Cyclohexane/EtOAc: 80/20) to yield pure Fmoc-ATC-*O*dimethylallyle **12e** as a clear oil. Yield 41% (952 mg). ^{1}H NMR (400 MHz, $CDCl_3$) δ 1.0 (d, J = 7.5 Hz, 6H, *i*Bu $\underline{CH_3}$); 1.48 (d, J = 6.7 Hz, 3H, $\underline{CH_3}$); 1.65 (s, 6H, dimethylallyl $\underline{CH_3}$); 2.11 (m, 1H, iBu $\underline{CH}$); 2.82 (d, J = 7.1 Hz, 2H, *i*Bu $\underline{CH}$);

4.23 (t, *J* = 7.00 Hz, 1H, Fmoc CH); 4.35 (m, 2H, Fmoc CH_2); 5.15 (d, *J* = 10.9 Hz, 1H, CH_2=CH); 5.27 (d, *J* = 17.3 Hz, 1H, CH_2=CH) 5.68 (m, 1H, CH-NH); 6.02 (d, *J* = 8.7 Hz, 1H, NH); 6.18 (dd, *J* = 10.9, 17.3 Hz, 1H, CH_2=CH); 7.29 (d, *J* = 7.6 Hz, 1H, Ar); 7.31 (d, *J* = 7.3 Hz, 1H, Ar); 7.39 (d, *J* = 7.6 Hz, 1H, Ar); 7.41 (d, *J* = 7.3 Hz, 1H, Ar); 7.59 (d, *J* = 4.9 Hz, 1H, Ar); 7.61 (d, *J* = 7.3 Hz, 1H, Ar); 7.76 (d, *J* = 7.6 Hz, 2H, Ar). ^{13}C NMR (100 MHz, $CDCl_3$) δ 22.3 (CH_3); 22.4 (2C, *i*Bu CH_3); 26.7 (2C, dimethylallyl CH_3); 29.9 (*i*Bu CH); 42.6 (*i*Bu CH_2); 46.7 (NH-CH); 47.4 (Fmoc CH); 66.8 (Fmoc CH_2); 83.1 (dimethylallyl $C(CH_3)_2$); 113.5 (CH_2=CH); 120.1 (2C, Ar); 122.7 (Ar); 125.3 (2C, Ar); 127.1 (2C, Ar); 127.7 (2C, Ar); 141.4 (2C, Ar); 142.0 (CH_2=CH); 144.2 (Ar); 144.3 (Ar); 155.7 (O-CO-N); 160.5 (COO); 162.5 (Thiaz C4); 174.0 (Thaz C2). LC Rt = 2.85 min. LC-MS: (ESI+): m/z 541.1 ($[M+Na]^+$) 40%, 519.1 ($[M+H]^+$) 85%, 451.1 ($[M-C_5H_9+2H]^+$) 100%. HRMS (ESI+) m/z calcd. for $[C_{30}H_{35}N_2O_4S]^+$: $[M+H]^+$ 519.2318, found 519.2318.

4-[(1*S*)-1-(N-Fmoc)-aminoethyl]-2-isobutyl-1,3-thiazole-5-carboxylatic acid (13e): The *O*-dimethylallylester **12e** (1.8 mmol) was dissolved in dry THF (10 mL). Tetrakis (triphenylphosphine)palladium(0) (3 mol %) was then added to the solution and the orange mixture was stirred for 5 min at r.t.. Then $PhSiH_3$ (1.2 equiv.) was added and the solution was stirred for 30 min (HPLC monitoring).

The solvent was then evaporated under vacuum to yield Fmoc-ATC-OH **13e** as a brown foam (1.25 g).). LC Rt = 2.23 min. LC-MS: (ESI+): m/z 451.2 ($[M+H]^+$) 100%.

***N*-Boc-aminovaleramide (15):** To a solution of 5-(Boc-amino)pentanoic acid **14** (1.0 equiv., 36.8 mmol, 8.0 g) in anhydrous THF at 0°C and under argon atmosphere were sequentially added IBCF (1.2 equiv.) and triethylamine (1.2 equiv.). The white suspension was stirred for 10 min until complete formation of the mixed anhydride (HPLC monitoring). Then gaseous ammonia was bubbled for 30 min at r.t. to yield *N*-Boc-aminovaleramide **15** as a white powder. Quantitative yield (8.02 g). ^{1}H NMR (400 MHz, DMSO-d_6) δ 1.37 (s, 9H, *t*Bu); 1.42-1.46 (m, 4H, CH_2-$\underline{CH_2}$-$\underline{CH_2}$-CH_2); 2.01 (t, *J* = 7.2 Hz, 2H, $\underline{CH_2}$-CO); 2.88 (m, 2H, NH-$\underline{CH_2}$); 6.68 (s, 1H, CO-$\underline{NH_2}$); 6.76 (t, 1H, *J* = 5.4 Hz, $\underline{NH}$); 7.21 (s, 1H, CO-$\underline{NH_2}$).

***N*-Boc-aminopentanethioamide (16): 15** (1.0 equiv., 36.8 mmol, 8.02 g) was dissolved in dry DCM (180 mL). Then Lawesson's reagent was added in one portion (0.55 equiv., 20.3 mmol, 8.19 g) and the white turbid mixture was heated at 32°C overnight. After evaporation under reduced pressure, the yellow oil was dissolved in a mixture of DCM (200 mL) and aqueous saturated $NaHCO_3$

solution (200 mL) which was stirred for 15 min. After transfer in a separating funnel, the organic layer was washed with brine, dried over $MgSO_4$, filtered and concentrated under reduced pressure to yield crude product (orange oil) which was purified by chromatography on silica gel (Et_2O/Petroleum ether: 5/5 to 9/1) to yield pure *N*-Boc-aminopenthanethioamide **16** as white solid. Yield 50 % (4.28 g). ^{1}H NMR (400 MHz, DMSO-d_6) δ 1.37 (s, 11H, *t*Bu and CH_2); 1.60 (quin, *J* = 7.5 Hz, 2H, H_4 or CH_2); 2.44 (t, *J* = 7.5 Hz, 2H, $\underline{CH_2}$-CS); 2.89 (m, 2H, NH-$\underline{CH_2}$); 6.78 (t, *J* = 5.4 Hz, 1H, $\underline{NH}$); 9.11 (s, 1H, CS-$\underline{NH_2}$); 9.31 (s, 1H, CS-$\underline{NH_2}$). LC Rt = 1.36 min. LC-MS: (ESI+): m/z 255.1 ($[M+Na]^+$) 90%, 233.1 ($[M+H]^+$) 25%, 133.1 ($[M-Boc+H]^+$) 100%.

1,1-dimethylprop-2-en-1-yl 4-[(1*S*)-1-(N-Fmoc)-aminoethyl]-2-(4-(Boc-amino)butyl)-1,3-thiazole-5-carboxylate (12f): A solution of **11a** (1.0 equiv., 1.95 mmol, 976 mg) and **16** (2.0 equiv.) in EtOH was stirred 90 min at r.t. then 30 min at 40°C. After evaporation of the solvent under reduced pressure, the crude was purified by flash chromatography (Cyclohexane/EtOAc: 90/10 to 60/40) to yield pure **12f** as a clear oil. Yield 56% (697 mg). ^{1}H NMR (400 MHz, $CDCl_3$) δ 1.44 (s, 9H, *t*Bu); 1.47 (d, *J* = 6.7 Hz, 3H, $\underline{CH3}$-CHNH); 1.59 (m, 2H, $\underline{CH_2}$-CH_2-NHBoc); 1.63 (s, 3H, dimethylallyl $\underline{CH_3}$); 1.65 (s, 3H, dimethylallyle $\underline{CH_3}$); 1.82 (quin, *J* = 7.6

Hz, 2H, $\underline{CH_2}$-CH_2-CH_2-NHBoc), 2.98 (t, *J* = 7.6 Hz, 2H, $\underline{CH_2}$-$(CH_2)_3$-NHBoc); 3.16 (brm, 2H, $\underline{CH_2}$-NHBoc); 4.22 (t, *J* = 7.1 Hz, 1H, Fmoc CH); 4.35 (d, *J* = 7.8 Hz 2H, Fmoc CH_2); 4.66 (br, 1H, $\underline{NH}$-Boc); 5.15 (d, *J* = 11.1 Hz, 1H, $\underline{CH_2}$=CH); 5.26 (d, *J* = 17.8 Hz, 1H, $\underline{CH_2}$=CH); 5.67 (m, 1H, $\underline{CH}$-NHFmoc); 6.02 (brm, 1H, $\underline{NH}$-Fmoc); 6.16 (dd, *J* = 11.1, 17.8 Hz, 1H, CH_2=$\underline{CH}$); 7.30 (m, 2H, Ar); 7.39 (t, *J* = 7.4 Hz, 2H, Ar); 7.61 (t, *J* = 7.7 Hz, 2H, Ar) ; 7.76 (d, *J* = 7.4 Hz, 2H, Ar). ^{13}C NMR (100 MHz, $CDCl_3$) δ 22.1 ($\underline{CH3}$-CHNH); 26.7 (2C, dimethylallyl $\underline{CH_3}$); 27.9 ($\underline{CH_2}$-CH_2-CH_2-NHBoc); 28.6 (3C, *t*Bu); 29.5 (C_{23}); 33.2 ($\underline{CH_2}$-$(CH_2)_3$-NHBoc); 40.2 ($\underline{CH_2}$-NHBoc); 46.7 ($\underline{CH_2}$-NHBoc); 47.4 ($\underline{CH}$ Fmoc); 66.9 ($\underline{CH_2}$ Fmoc); 79.4 (*t*Bu); 83.2 (CH_2=CH-$\underline{C}$); 113.6 ($\underline{CH_2}$=CH); 120.1 (2C, Ar); 122.8 (S-$\underline{C}$-CO); 125.3 (2C, Ar); 127.1 (2C, Ar); 127.8 (2C, Ar); 141.4 (2C, Ar); 142.0 (CH_2=$\underline{CH}$); 144.1 (Ar); 144.3 (Ar); 155.7 (FmocNH-$\underline{CO}$); 156.1 (BocNH-$\underline{CO}$); 160.4 (S-C-$\underline{CO}$); 162.6 ($\underline{C}$-CH(CH_3)-NH); 174.5 (S-$\underline{C}$-N). LC Rt = 2.62 min. LC-MS: (ESI+): m/z 656.1 ($[M+Na]^+$) 25%, 634.1 ($[M+H]^+$) 100%, 578.0 ($[M-t\text{Bu}+2H]^+$) 30%, 534.1 ($[M\text{-Boc}+H]^+$) 80%, 466.0 ($[M\text{-Boc-}C_5H_9+H]^+$) 55%. HRMS (ESI+) m/z calcd. for $[C_{35}H_{44}N_3O_6S]^+$: $[M+H]^+$ 634.2949, found 634.2951.

4-[(1*S*)-1-(N-Fmoc)-aminoethyl]-2-(4-(Boc-amino)butyl)-1,3-thiazole-5-carboxylic acid (13f): The *O*-dimethylallylester **12f** (1.10 mmol) was dissolved in

dry THF (5 mL). Tetrakis (triphenylphosphine)palladium(0) (3 mol %) was then added to the solution and the orange mixture was stirred for 5 min at r.t.. Then $PhSiH_3$ (1.2 equiv.) was added and the solution was stirred for 30 min (HPLC monitoring). The solvent was then evaporated under vacuum to yield Fmoc-ATC-OH **13f** as a brown foam (630 mg).). LC Rt = 2.12 min. LC-MS: (ESI+): m/z 588.2 ($[M+Na]^+$ 20%, 566.2 ($[M+H]^+$) 30%, 466.2 ($[M-Boc+H]^+$) 100%.

1,1-dimethylprop-2-en-1-yl 4-[(1*S*)-1-(N-Fmoc)-amino-3-methylbutyl]-2-(4-(Boc-amino)butyl)-4-hydroxy-4,5-dihydrothiazole-5-carboxylate (17): 16 (1.1 equiv., 5.41 mmol, 1.26 g) was dissolved in DME (35 mL) and then $KHCO_3$ (8.0 equiv., 39.3 mmol, 3.93 g) was added in one portion. The mixture was vigorously stirred for 30 min at r.t.. **11b** was dissolved in 40 mL of DME and added to the mixture with a dropping funnel at 0°C. The reaction was stirred overnight at r.t.. The crude was filtered to remove undissolved $KHCO_3$ and the clear filtrate was evaporated under reduced pressure. The resulting yellow oil was dissolved in EtOAc (100 mL) then washed with water (1 × 100 mL) and brine (1 × 50 mL), dried over $MgSO_4$ and filtered. The solvent was evaporated to yield the corresponding thiazoline **17** as an orange foam. Quantitative yield (3.44 g). LC Rt = 2.57 min. LC-MS: (ESI+): m/z 694.3 ($[M+H]^+$) 100%.

1,1-dimethylprop-2-en-1-yl 4-[(1*S*)-1-(N-Fmoc)-amino-3-methylbutyl]-2-(4-(Boc-2,2,2-trifluoroacetamido)butyl)-1,3-thiazole-5-carboxylate (18): The thiazoline **17** was dissolved in 50 mL of dry THF at -15°C. Di*iso*proylethylamine (8.0 equiv., 39.3 mmol, 6.80 mL) was added and the mixture was stirred for 15 min. Then trifluoroacetic anhydride (4.0 equiv., 19.6 mmol, 2.74 mL) was added dropwise (4-5 min). After 10 min of stirring at -15°C the mixture was diluted with DCM (100 mL) and washed with aqueous saturated $NaHCO_3$ solution (2 × 100 mL), then with aqueous saturated $KHSO_4$ solution (1 × 100 mL) and brine (1 × 50 mL). The organic layer was dried over $MgSO_4$, filtered and concentrated under reduced pressure to yield 4.19 g of -15°C **18** as a red foam.

1,1-dimethylprop-2-en-1-yl 4-[(1*S*)-1-(N-Fmoc)-amino-3-methylbutyl]-2-(4-(Boc-amino)butyl)-1,3-thiazole-5-carboxylate (12g): $KHCO_3$ (2.0 equiv., 9.82 mmol, 983 mg) was added to a solution of **18** dissolved in dry MeOH (50 mL). The suspension was stirred overnight at r.t. then diluted with DCM (80 mL) and washed with aqueous saturated $NaHCO_3$ solution (1 × 50 mL) and brine (2 × 70 mL). The organic layer was dried over $MgSO_4$, filtered, concentrated under reduced pressure and filtered through a Celite pad to yield crude **12g** as an orange foam which was used for the next step without further purification. Yield

93% (3.09 g). ^{1}H NMR (400 MHz, $CDCl_3$) δ 0.95 (d, *J* = 6.4 Hz, 3H, CH_3-CH-CH_3); 0.97 (d, *J* = 6.4 Hz, 3H, CH_3-CH-CH_3); 1.44 (s, 9H, *t*Bu); 1.55-1.62 (m, 3H, CH_2(*i*Pr) and CH_2-CH_2-NHBoc); 1.66 (s, 7H, dimethylallyl CH_3 and CH_3-CH-CH_3); 1.70-1.83 (m, 3H, CH_2(*i*Pr) and CH_2-CH_2-CH_2-NHBoc); 2.96 (t, *J* = 7.6 Hz, 2H, CH_2-$(CH_2)_3$-NHBoc); 3.15 (brm, 2H, CH_2-NHBoc); 4.21 (t, *J* = 7.0 Hz, 1H, CH Fmoc); 4.30 (dd, *J* = 7.5, 10.5 Hz, 1H, CH_2 Fmoc); 4.39 (dd, *J* = 7.5, 10.5 Hz 1H, CH_2 Fmoc); 4.67 (brm, 1H, NHBoc); 5.14 (d, *J* = 11.0 Hz, 1H, CH_2=CH); 5.26 (d, *J* = 17.5 Hz, 1H, CH_2=CH); 5.70 (m, 1H, Fmoc-NH-CH); 5.84 (brm, 1H, Fmoc-NH); 6.19 (dd, *J* = 11.0, 17.5 Hz, 1H, CH_2=CH); 7.29 (m, 2H, Ar); 7.38 (t, *J* = 7.3 Hz, 2H, Ar); 7.58 (d, *J* = 7.1 Hz, 1H, Ar); 7.59 (d, *J* = 5.3 Hz, 1H, Ar) 7.75 (d, *J* = 7.3 Hz, 2H, Ar). ^{13}C NMR (100 MHz, $CDCl_3$) δ 22.3 (CH_3-CH-CH_3); 23.3 (CH_3-CH-CH_3); 25.1 (CH_3-CH-CH_3); 26.7 (dimethylallyl CH_3); 26.8 (dimethylallyl CH_3); 27.1 (CH_2-CH_2-CH_2-NHBoc); 28.5 (3C, *t*Bu); 29.5 (CH_2-CH_2-NHBoc); 33.2 (CH_2-$(CH_2)_3$-NHBoc); 40.2 (CH_2-NHBoc); 45.2 (CH_2(*i*Pr)); 47.4 (CH Fmoc); 49.0 (FmocNH-CH); 66.7 (CH_2 Fmoc); 79.4 (*t*Bu); 83.3 (CH_2=CH-C); 113.5 (CH_2=CH); 120.1 (2C, Ar); 123.4 (S-C-CO); 125.3 (2C, Ar); 127.1 (2C, Ar); 127.7 (2C, Ar); 141.4 (2C, Ar); 142.1 (CH_2=CH); 144.1 (Ar); 144.2 (Ar); 155.9 (NH-CO Fmoc); 156.1 (NH-CO Boc); 160.5 (S-C-CO); 162.3 (S-C-C-N); 174.4 (S-C-N). LC Rt = 2.92 min. LC-MS: (ESI+): m/z

698.2 ([M+Na]$^+$) 55%, 676.2 ([M+H]$^+$) 100%, 576.1 ([M-Boc+2H]$^+$) 75%, 508.1 ([M-C_5H_9+2H]$^+$), 50%. HRMS (ESI+) m/z calcd. for $[C_{38}H_{50}N_3O_6S]^+$: [M+H]$^+$ 676.3421, found 676.3420.

4-[(1*S*)-1-(N-Fmoc)-amino-3-methylbutyl]-2-(4-(Boc-amino)butyl)-1,3-thiazole-5-carboxylic acid (13g): The *O*-dimethylallylester **12g** (4.5 mmol) was dissolved in dry THF (25 mL). Tetrakis (triphenylphosphine)palladium(0) (3 mol %) was then added to the solution and the orange mixture was stirred for 5 min at r.t.. Then $PhSiH_3$ (1.2 equiv.) was added and the solution was stirred for 30 min (HPLC monitoring). The solvent was then evaporated under vacuum to yield Fmoc-ATC-OH **13g** as a brown foam (1.25 g). LC Rt = 2.34 min. LC-MS: (ESI+): m/z 630.2 ([M+Na]$^+$) 5%, 608.2 ([M+H]$^+$) 25%; 552.1 ([M-*t*Bu+2H]$^+$) 15%; 508.1 ([M-Boc+2H]$^+$) 100%.

4-(Boc-amino)butanamide (20): To a solution of 4-(Boc-amino)butanoic acid **19** (1.0 equiv., 60 mmol, 12.2 g) in anhydrous THF at 0°C and under argon atmosphere were sequentially added ethylchloroformate (1.2 equiv.) and triethylamine (1.2 equiv.). The white suspension was stirred for 10 min until complete formation of the mixed anhydride (HPLC monitoring). Then gaseous ammonia was bubbled for 30 min. THF was evaporated, the resulting product

was diluted in DCM and 2M $KHSO_4$. The organic layer was washed with 2M $KHSO_4$ and brine, dried on $MgSO_4$, filtered and evaporated to yield the crude product which was used in the next step without further purification. Yield 98%. ^{1}H NMR (400 MHz, $CDCl_3$) δ 1.43 (s, 9H, H_9); 1.79 (quin, *J* = 7.1 Hz, 2H, H_4); 2.26 (t, *J* = 7.1 Hz, 1H, H_3); 2.36 (t, *J* = 7.1 Hz, 1H, H_3); 3.17 (brm, H, H_5); 3H missing.

4-(Boc-amino)butanethioamide (21): 20 (1.0 equiv., 55.1 mmol, 11.1 g) was dissolved in dry THF (150 mL) and Lawesson's reagent (0.55 equiv., 30.3 mmol, 12.25 g) was then added in one portion. The mixture was stirred at room temperature for 30 min (CCM monitoring, silica gel, AcOEt 100%). An aqueous saturated solution of $NaHCO_3$ (70 ml) was then added to the reaction mixture. The solution was stirred at room temperature over 1.5h then DCM (200 ml) was added to the mixture. After transfer in a separating funnel, the organic layer was washed with an aqueous saturated solution of $NaHCO_3$ (2x300 ml) then brine. The organic layer was dried over $MgSO_4$, filtered and concentrated under reduced pressure to yield crude product (yellow oil). Purification by chromatography on silica gel (Cyclohexane/EtOAc: 60/40 to 30/70 over 10 CV) to yield pure **21** as slight yellow crystals. Yield 38 % (4.94 g). ^{1}H NMR (400 MHz, $CDCl_3$) δ 1.43 (s, 9H, *t*Bu); 1.60 (quin, *J* = 6.2 Hz, 2H, NH-CH_2-$\underline{CH_2}$); 2.72 (t, *J* = 6.2

Hz, 2H, $\underline{CH_2}$-CS); 3.21 (q, *J* = 6.4 Hz, 2H, NH-$\underline{CH_2}$); 4.79 (br, 1H, NH); 7.64 (br, 1H, NH); 8.71 (br, 1H, NH). LC Rt = 1.24 min. LC-MS: (ESI+): m/z 241.1 ($[M+Na]^+$) 5%, 219.1 ($[M+H]^+$) 20%, 163.1 ($[M-t\text{Bu}+2H]^+$) 100%, 119.1 ($[M-\text{Boc}+2H]^+$) 45%.

4-aminobutanethioamide, HCl (22): A solution of 6N HCl in 1,4-dioxane (50 mL)was added to **21** (1.0 equiv., 22.4 mmol, 4.89 g) and the mixture was stirred for 1 h at r.t. The reaction was monitored by HPLC. The solvent was evaporated *in vacuo*. Co-evaporation with MeOH yielded **22** as a yellow oil. Quantitative yield (3.76 g). LC Rt = 0.30 min (≥ 95%). LC-MS: (ESI+): m/z 118.9 ($[M+H]^+$) 100%.

1,3-Di-Boc-guanidine (24): 1,4-dioxane (80 mL) was added to a solution of guanidine hydrochloride (1.0 eq, 40 mmol) and sodium hydroxide (4.0 eq) dissolved in water (40 mL) and the resulting mixture was cooled to 0°C. Boc_2O (2.2 eq) was added in one portion and the reaction mixture was stirred to room temperature overnight. Mixture was concentrated in vacuo to one third of its original volume. The resulting suspension was diluted with water and extracted with AcOEt. The combined organic layers were washed with 10% citric acid, water and brine. The organic layer was dried on MgSO4, filtered and the solvent was removed under vacuum to give the crude product which was used in the

next step without further purification. If necessary the crude could be purified by chromatography on silica gel (DCM/MeOH 99/1 to 96/4) to yield **23** as a white powder. Yield 53%. ^{1}H NMR (400 MHz, $CDCl_3$) δ 1.41 (s, 18H, *t*Bu); 8.48 (br, 1H, =NH); 10.35 (br, 2H, NH-C-NH). LC Rt = 1.48 min (≥ 95%). LC-MS: (ESI+): m/z 260.1 ($[M+H]^+$) 70%, 204.3 ($[M-t\text{Bu}+2H]^+$) 90%, 147.6 ($[M-2t\text{Bu}+3H]^+$) 100%.

1,3-Di-Boc-2-(trifluoromethylsulfonyl)guanidine (25): A solution of **24** (1.0 equiv., 21 mmol, 5.44 g) and trimethylamine (1.08 equiv., 22.7 mmol, 3.1 mL) in anhydrous DCM (105 mL) was cooled to -78°C under an argon atmosphere. Triflic anhydride (1.05 equiv., 22.0 mmol, 3.71 mL) was added dropwise at a rate such that reaction temperature does not exceed -70°C. After the addition was completed, the reaction mixture was allowed to warm to room temperature within 4 hours. The solution was transferred to a separation funnel, washed with 2N $KHSO_4$ and water and dried over magnesium sulfate. The organic layer was dried over $MgSO_4$, filtered and concentrated under reduced to yield crude **25** as a slight yellow powder which was used for the next step without further purification. If necessary the crude could be purified by flash column chromatography (Silica gel, Hex/AcOEt). Yield 89% (7.3 g). ^{1}H NMR (400 MHz,

$CDCl_3$) δ 1.46 (s, 18H, *t*Bu); 11.05 (br, 2H, NH-C-NH). LC Rt = 2.26 min (≥ 95%). LC-MS: (ESI+): m/z 392.0 ($[M+H]^+$) 5%, 336.1 90%, 280.1 95%, 236.2 100%.

1,2-Di-Boc-3-guanidinopropylthioamide (26): 22 (1.1 equiv., 20.35 mmol, 3.15 g) was dissolved in a 1:1 mixture of DCM: MeOH (80mL) and added in one time to a solution of **25** (1.0 equiv., 18.5 mmol, 7.24 g) and triethylamine (1.0 equiv., 18.5 mmol, 2.53 mL) dissolved in DCM (80 mL). After 80 min of stirring at r.t., reaction was stopped. Mixture was diluted with DCM (60 mL) and washed with water (100 mL), $KHSO_4$ (100 mL), $NaHCO_3$ (100 mL) and brine (100 mL). After filtering and removal of the solvent under reduced pressure, crude was purified by flash chromatography on silica gel (Cyclohexane/EtOAc 90/10 to 65/35) to yield pure **26** as a white powder. Yield 47% (3.14 g). ^{1}H NMR (400 MHz, $CDCl_3$) δ 1.44 (s, 9H, *t*Bu); 1.49 (s, 9H, *t*Bu); 1.96 (m, 2H, CH_2-CH_2-CS); 2.81 (m, 2H, CH_2-CS); 3.44 (q, *J* = 6.1 Hz, 2H, NH-CH_2); 7.72 (br, 1H, NH-Boc); 8.58 (t, *J* = Hz, 1H, NH-CH_2); 10.41 (br, 1H, CS-NH); 11.36 (br, 1H, CS-NH). ^{13}C NMR (100 MHz, $CDCl_3$) δ 28.1 (3C, *t*Bu); 28.3 (3C, *t*Bu); 29.4 (CH_2-CH_2-CS); 39.0 (NH-CH_2); 43.4 (CH_2-CS); 79.9 (C-$(CH_3)_3$); 83.9 (C-$(CH_3)_3$); 153.2 (C=O); 157.3 (N-C-N); 162.5 (C=O); 209.4 (CS). LC Rt = 1.65 min. LC-MS: (ESI+): m/z 361.0 ($[M+H]^+$) 100%, 305.1 ($[M-t\text{Bu}+2H]^+$) 100%, 249.1 ($[M-2t\text{Bu}+3H]^+$) 65%, 205.1 ($[M-2t\text{Bu-Boc}+4H]^+$)

30%. HRMS (ESI+) m/z calcd. for $[C_{15}H_{29}N_4O_4S]^+$: $[M+H]^+$ 361.1910, found 361.1910.

1,1-dimethylprop-2-en-1-yl 4-[(1*S*)-1-(N-Fmoc)-aminoethyl]-2-(3-(2,3-Di-Boc-guanidino)propyl)-4-hydroxy-4,5-dihydrothiazole-5-carboxylate (27): To a solution of thioamide **26** (1.2 eq, 10 mmol) in DME (160 ml) was added $KHCO_3$ in one portion (8.0 eq). The mixture was stirred for 30 minutes at r.t. A solution of α-bromo-β-ketoester **11a** (1 eq, 8. 3 mmol) in DME (100 ml) was added to the mixture dropwise at 0°C. The reaction was stirred overnight at r.t.. The crude was filtered to remove undissolved $KHCO_3$ and the clear filtrate as evaporated. Resulting yellow oil was dissolved in AcOEt and washed with water and brine, dried on $MgSO_4$, filtered and evaporated to quantitatively yield the thiazoline **27**.

1,1-dimethylprop-2-en-1-yl 4-[(1*S*)-1-(N-Fmoc)-aminoethyl]-2-(3-(2,3-Di-Boc-guanidino)propyl)-1,3-thiazole-5-carboxylate (12h): To a solution of thiazoline **27** (1 eq, 8.93 mmol) in dry THF (100 ml) was added DIEA (4 eq) and DMAP (0.5 eq) at 0°C. Trifluoroacetic anhydride (2 eq), dissolved in 45 mL of dry THF, was added dropwise over 30 minutes. The reaction was completed after 15 minutes stirring at 0°C. The mixture was diluted in DCM and washed with water,

saturated aqueous $NaHCO_3$ solution, K_2SO_3 solution and brine. The organic layer was dried on $MgSO_4$, filtered and evaporated under vacuum to yield the crude product. The crude was purified by flash column chromatography (Silica gel, DCM 100% to DCM/AcOEt 8:2 over 10 CV). Yield = 27%. ^{1}H NMR (400 MHz, $CDCl_3$) δ 1.48 (brm, 3H, $\underline{CH_3}$-CH); 1.50 (s, 18H, *t*Bu); 1.63 (m, 6H, CH_3 dimethylallyl); 2.08 (t, *J* = 7.2 Hz, 1H, $\underline{CH_2}$-CH_2NH); 3.03 (t, *J* = 7.6 Hz, 2H, $\underline{CH_2}$-$(CH_2)_2$NH); 3.53 (brm, 2H, $\underline{CH_2}$-NH); 4.22 (t, *J* = 7.1 Hz, 1H, CH Fmoc); 4.33 (d, *J* = 7.1 Hz, 2H, CH_2 Fmoc); 5.14 (dd, *J* = 10.9, 0.7 Hz, 1H, $\underline{CH_2}$=CH minor conformer); 5.15 (d, *J* = 10.9 Hz, 1H, $\underline{CH_2}$=CH, major conformer); 5.24 (d, J = 17.4 Hz, 1H, $\underline{CH_2}$=CH, minor conformer); 5.26 (d, *J* = 17.4 Hz, 1H, $\underline{CH_2}$=CH, major conformer) 5.69 (m, 1H, CH_3-$\underline{CH}$-NH); 6.02 (d, *J* = 9.3 Hz, 1H, $\underline{NH}$-Fmoc); 6.16 (m, 1H, CH_2=$\underline{CH}$); 7.29 (td, *J* = 7.4, 2.2 Hz, 2H, Ar); 7.38 (t, *J* = 7.5 Hz, 2H, Ar); 7.59 (d, *J* = 6.7 Hz, 1H, Ar); 7.61 (d, *J* = 6.7 Hz, 1H, Ar); 7.75 (d, *J* = 7.5 Hz, 2H, Ar). ^{13}C NMR (100 MHz, $CDCl_3$) δ 22.2 ($\underline{CH_3}$-CH); 26.7 (2C, CH_3 dimethylallyl); 28.2 (3C, *t*Bu); 28.5 (3C, *t*Bu); 29.0 ($\underline{CH_2}$-CH_2NH); 30.8 ($\underline{CH_2}$-$(CH_2)_2$NH); 39.8 ($\underline{CH_2}$-NH); 46.7 ($\underline{CH}$-NHFmoc); 47.4 (CH Fmoc); 66.9 (CH_2 Fmoc); 79.5 (*t*Bu); 83.2 (C-$(CH_3)_3$); 83.4 (C-$(CH_3)_3$); 113.6 ($\underline{CH_2}$=CH); 120.1 (2C, Ar); 122.9 (S-$\underline{C}$-CO); 125.3 (2C, Ar); 127.1 (2C, Ar); 127.7 (2C, Ar); 141.4 (2C, Ar); 142.0 (CH_2=$\underline{CH}$); 144.1 (Ar); 144.3 (Ar);

153.4 (N-CO-Boc); 155.7 (N-CO-Fmoc); 156.4 (NH-C-NH); 160.3 (S-C-CO); 162.8 (S-C-C-N); 163.8 (N-CO-Boc); 173.4 (S-C-N). LC Rt = 2.58 min. LC-MS: (ESI+): m/z 762.4 ($[M+H]^+$) 100%, 662.3 ($[M-Boc+2H]^+$) 75%, 562.2 ($[M-2Boc+3H]^+$) 20%. HRMS (ESI+) m/z calcd. for $[C_{40}H_{52}N_5O_8S]^+$: $[M+H]^+$ 762.3543, found 762.3537.

4-[(1*S*)-1-(N-Fmoc)-aminoethyl]-2-(3-(2,3-Di-Boc-guanidino)propyl)-1,3-thiazole-5-carboxylic acid (13h): The *O*-dimethylallylester **12h** (1.3 mmol) was dissolved in dry THF (5 mL). Tetrakis (triphenylphosphine)palladium(0) (3 mol %) was then added to the solution and the orange mixture was stirred for 5 min at r.t.. Then $PhSiH_3$ (1.2 equiv.) was added and the solution was stirred for 30 min (HPLC monitoring). The solvent was then evaporated under vacuum to yield Fmoc-ATC-OH **13h** as a brown foam (1.25 g) which was used without further purification. LC Rt = 2.18 min. LC-MS: (ESI+): m/z 694.2 ($[M+H]^+$) 100%, 594.2 ($[M-Boc+2H]^+$) 40%, 494.2 ($[M-2Boc+3H]^+$) 5%.

γ-peptide oligomerization: Solid-phase syntheses were performed on a ChemMatrix® Rink Amide resin loaded at 0.49 mmol/g using Fmoc/*t*-Bu chemistry. Resin was swollen in *N*-methylpyrrolidone (NMP) for 5-10 minutes and filtered. Fmoc-ATC-OH (1.5 equiv.), DIC (1.5 equiv.), Oxyma Pure (1.5 equiv.) in NMP (2.5 ml for 0.25 mmol of resin) were added in this order for each

peptide coupling (overnight at r.t.). Resin was washed using the following procedure: 3 × DMF, 3 × DCM, 3 × MeOH, 1 × DMF, 1 × MeOH, 1 × DCM. Each coupling was followed by a capping step with a Ac_2O/DCM 1/1 vv solution (1 × 5 min at r.t.) and washed. Fmoc removal was performed using a 20% piperidine/DMF solution (3 × 10 min at r.t.) and the resin was then washed before the next coupling. Deprotection and coupling steps were monitored by Kaiser test. After completion of the oligomerization process, the foldamer was *N*-deprotected (3 × 10 min at r.t.), capped with a Ac_2O/DCM 1/1 vv solution (2 × 5 min at r.t.) and cleaved from the resin with a TFA/TIS/H_2O 95/2.5/2.5 vvv solution (2 × 90 min at r.t.). The resin was washed (1 × DCM). The filtrate was evaporated under reduced pressure. The crude peptide was precipitated with cold diethylether, centrifugated 10 min at 5°C and lyophilized. Purifications by preparative RP-HPLC were performed on a Waters system controller equipped with a C_{18} Waters Delta-Pack column (100 × 40 mm, 100 Å) flow 50 mL/min; UV detection at 214 nm using a Waters 486 Tunable Absorbance Detector and a linear gradient of A = H_2O (0.1 % TFA) and B = CH_3CN (0.1 % TFA). Characterizations of oligomers **1-9** are reported in the Supporting information.

NMR experiments: 3, 4 (2-4 mM) were dissolved in H_20/D_2O (pH 6.5) while **6, 7, 8** and **9 (**2-4 mM) were dissolved in CD_3OH. All spectra were recorded on a Bruker Avance 600 AVANCE III spectrometer equipped with a 5 mm triple-resonance cryoprobe (^1H, ^{13}C, ^{15}N). Homonuclear 2-D spectra DQF-COSY, TOCSY (DIPSI2) and ROESY were typically recorded in the phase-sensitive mode using the States-TPPI method as data matrices of 256-512 real (t_1) × 2048 (t_2) complex data points; 8-48 scans per t_1 increment with 1.0 s recovery delay and spectral width of 6009 Hz in both dimensions were used. The mixing times were 60 ms for TOCSY and 350-450 ms for the ROESY experiments. In addition, 2D heteronuclear spectra ^{15}N, ^{13}C-HSQC and ^{13}C-HSQC-TOCSY were acquired to fully assign the oligomers (8-32 scans, 256-512 real (t_1) × 2048 (t_2) complex data points). Spectra were processed with Topspin (Bruker Biospin) and visualized with Topspin or NMRview on a Linux station. The matrices were zero-filled to 1024 (t_1) x 2048 (t_2) points after apodization by shifted sine-square multiplication and linear prediction in the F1 domain. Chemical shifts were referenced to the solvent.

Molecular modelling studies: ^1H chemical shifts were assigned according to classical procedures. NOE cross-peaks were integrated and assigned within the

NMRView software.[54] The volume of a ROE between methylene pair protons was used as a reference of 1.8 Å. The lower bound for all restraints was fixed at 1.8 Å and upper bounds at 2.7, 3.3 and 5.0 Å, for strong, medium and weak correlations, respectively. Pseudo-atoms corrections of the upper bounds were applied for unresolved aromatic, methylene and methyl protons signals as described previously.[55] Structure calculations were performed with AMBER 16[43] in two stages: cooking and simulated annealing with the generalized Born (GB) implicit solvent model. The cooking stage was performed at 1000 K to generate 100 initial random structures. SA calculations were carried during 20 ps (20000 steps, 1 fs long) as described elsewhere. First, the temperature was risen quickly and was maintained at 600 K for the first 5000 steps, then the system was cooled gradually from 600 K to 100 K from step 5001 to 18000 and finally the temperature was brought to 0 K during the 2000 remaining steps. For the 3000 first steps, the force constant of the distance restraints was increased gradually from 2.0 kcal.mol^{-1}.Å to 20 kcal.mol^{-1}.Å. For the rest of the simulation (step 3001 to 20000), the force constant is kept at 20 kcal.mol^{-1}.Å. The calculations were launched in vacuum. The 10 lowest energy structures with no violations > 0.3 Å

were considered as representative of the peptide structure. The representation and quantitative analysis were carried out using MOLMOL[56] and Chimera.[57]

DFT calculations: All DFT calculations have been performed using the hybrid-*meta*-GGA M06-2X functional[58] implemented in the Gaussian 09 program.[44] The lowest-energy NMR structure of compound **3** has been further optimized at the M06-2X/6-31G(d) level of theory in water using the solvation model based on density (SMD)[59] method and its electrostatic potential was calculated using the Merz-Singh-Kollman[60, 61] scheme at the same level of theory in water.

Microbiology

Antimicrobial activity: the antimicrobial performances of oligomers antimicrobial activity were determined on three Gram positive strains (*Bacillus subtilis ATCC6633*, *Staphylococcus aureus* ATCC6538 and *Enterococcus faecalis ATCC29121*), two Gram negative strains (*Escherichia coli* ATCC8739 *and Pseudomonas aeruginosa ATCC9027*) and one fungal strain (*Candida albicans ATCC10231*). Assays were carried out in duplicate on three independent experiments. Each bacterial strain was allowed to grow overnight on Trypto-Caseine-Soja agar (TSA, Difco) at 37°C. *C. albicans* was allowed to grow 48h on a sabouraud medium (Difco) at 20-25°C. A fresh suspension at 10^8 CFU.mL^{-1} was

then prepared by inoculating the micro-organisms in a Tryptone-Sel solution. Concentration was monitored by measuring transmitted light at 620 nm or with the Mac Farland turbidity standard (Mac Farland = 0.5 ≈ 10^8 CFU.mL^{-1}). Each suspension was then diluted in a doubly strong Mueller-Hinton (MH, Difco) broth to 10^6 CFU.mL^{-1}. Two-fold serial dilutions (100 μL) of oligomers in sterile water (pH adjusted between 7.4 and 7.7 with HCl and NaOH solutions) were mixed with microbial inoculum (100 μL) in NUNC sterile clear polystyrene flat-bottom 96-well plates. A 1/1 v/v oligomer solution/water mixture was used a negative control and a 1/1 vv water/microbial inoculum mixture was used a positive control. Plates were then incubated 24 h at 37°C for bacteria and 48 h at 25°C for *C. albicans*. Minimum Inhibitory Concentration (MIC) was determined as the lowest concentration inhibiting the growth of each micro-organism. After MIC determination, each well was transferred to a Petri dish containing MH agar, using a Mic-2000 inoculator (Dynatech) and was incubated 24 h at 37°C for bacteria and 48 h at 25°C for C. albicans. Minimum Bactericidal Concentration (MBC) was determined as the lowest concentration that prevent the growth of more than one colony. Each assay was performed in a triple duplicate for each strain.

Time-kill study: the antimicrobial kinetics of **8** were evaluated at 0, 1.8 μM (MIC), 7.2 μM (4xMIC) and 14.4 μM (8xMIC) and time intervals of 0, 10, 20, 40, 60 and 120 min. Briefly, a 10^6 CFU.mL^{-1} *E.coli* suspension was prepared in TS medium as previously described. Given concentrations of oligomer **8** were added in different bottle before incubation at 37°C, under shaking conditions (100 rpm). Samples of 100 μL were taken from each bottle at determined time intervals. Serial 10-fold dilutions in 0.9% sterile saline solution were prepared. Volumes of 100 μL from each dilution were plated in on TS agar for further CFU counting after 24 h incubation at 37°C.

Measurements of hemolytic activity: Human red blood cells (hRBCs) were washed multiple times with phosphate-buffered saline (PBS) until a clear supernatant was obtained. The hRBCs suspension was made in PBS with a Packed Cell Volume of 5%. Two-fold serial dilutions (50 μL) of oligomers in sterile PBS (pH adjusted between 7.4 and 7.7 with HCl and NaOH solutions) were mixed with hRBCs suspension (50 μL) in clear polystyrene optical-bottom 96-well plates which were filmed and incubated for 1 h at 37°C. A 1/1 vv hRBCs solution/PBS mixture was used a negative control and a 1/1 vv hRBCs solution /1% (TRIS 50 mM pH= 8.0 + 1% SDS) mixture was used a positive control for

100% hemolysis. The mixture was then centrifuged at 1500g for 10 min at 5°C. Next, 50 μL of the supernatant was transferred into a second plate, and the absorbance was read at 490 nm using a BioRad iMark plate reader. The hemolysis percentage was calculated by the formula % hemolysis = [Absorbance (sample)-Absorbance (negative control)]/[Absorbance (positive control)-Absorbance (negative control)] x 100. Each assay was performed in a double duplicate. Hemolytic activity was determined or estimated from three independent experiments with the Hemolytic Concentration leading to 50% of lysis of hRBCs (HC_{50}).

Surface electron microscopy: compound **8** (1.8 μM and 14.4 μM) was added to 1 mL of an overnight *E.coli* culture. An untreated culture was prepared as negative control. Treated and untreated samples were incubated for 60 min at 37°C. 200μL of cells were fixed with 2.5% glutaraldehyde in PHEM buffer, pH 7.2 for an hour at room temperature, followed by washing in PHEM buffer. PBS washed cells were fixed with 2.5% glutaraldehyde in PHEM buffer, pH 7.2 for an hour at room temperature, followed by washing in PHEM buffer. Fixed samples were dehydrated using a graded ethanol series (30-100%), followed by 10 minutes in graded Ethanol - Hexamethyldisilazane. And then

Hexamethyldisilazane alone. Subsequently, the samples were sputter coated with an approximative 10nm thick gold film and then examined under a scanning electron microscope (Hitachi S4000, at CoMET, MRI-RIO Imaging, Biocampus, INM Montpellier France) using a lens detector with an acceleration voltage of 10KV at calibrated magnifications.

Membrane depolarization experiments: Cytoplasmic membrane depolarization assays were carried out in duplicate on three independent experiments.[62] *E. coli* ATCC8739 strain was grown in 20mL Mueller Hinton broth for 2h at 37°C and centrifuged (2500g for 10 min at room temperature). The pellet was washed twice with 5mL of a buffer containing 20mM glucose and 5mM HEPES pH 7.2. Cells were suspended in the same buffer to an OD^{600} of 0.05. The fluorescent dye 3,3'-dipropylthiadicarbocyanine iodide (diSC3–5) (30μM prepared in DMSO) was added to the bacteria (0,6μM final concentration). The suspension was mixed by short vortexing then dispensed into a black 96-well plate (100 μl per well). The mixture was pre-incubated at 37°C until the fluorescence level stabilized then 100 μl of a solution of the tested compound was added (0.19 to 12.5 μM final concentration). Monitoring of the fluorescence (λex=620 nm, λem=670 nm) was performed over 30 min.

ASSOCIATED CONTENT

Supporting Information

Detailed synthetic procedures and analytical descriptions of the N-Fmoc-ATC-OH and oligomers **3-9** are reported in the SI. The coordinates of the lowest energy structure of **3** optimized at the SMD M06-2X/6-31G(d) level of theory in water is accessible in a 3-lowest-NRJ-w-m1-o.pdb file. Molecular formula strings of **1-9** are reported in the jm-2020-00077k mfs.csv file.

AUTHOR INFORMATION

Corresponding Author

* E-mail: ludovic.maillard@umontpellier.fr; patricia.licznar-fajardo@umontpellier.fr

Present Addresses

† Sygnature Discovery Ltd., 2 Pennyfoot Street, Biocity, Nottingham, NG1 1GR, United Kingdom

Author Contributions

The manuscript was written by L. T. Maillard. / All authors have given approval to the final version of the manuscript. / ‡ C. Bonnel is the main contributor.

ACKNOWLEDGMENT

The authors are grateful to Chantal Cazevieille for her technical assistance and interpreting data concerning ultrastructural evaluation.

ABBREVIATIONS

AMPs, Antimicrobial Peptides; ATC, 4-amino(methyl)-1,3-thiazole-5-carboxylic acid; CD, circular dichroism; SEM, surface electron microscopy.

REFERENCES

(1) Bahar, A. A.; Ren, D. Antimicrobial Peptides. Pharmaceuticals 2013, 6, 1543-1575.

(2) Hancock, R. E.; Sahl, H. G. Antimicrobial and Host-Defense Peptides as New Anti-Infective Therapeutic Strategies. *Nat. Biotechnol.* **2006,** 24, 1551-1557.

(3) Hancock, R. E.; Lehrer, R. Cationic Peptides: A New Source of Antibiotics. *Trends Biotechnol.* **1998,** 16, 82-88.

(4) Zasloff, M. Antimicrobial Peptides of Multicellular Organisms. *Nature* **2002,** 415, 389-395.

(5) Hancock, R. E.; Diamond, G. The Role of Cationic Antimicrobial Peptides in Innate Host Defences. *Trends Microbiol.* **2000,** 8, 402-410.

(6) Nicolau B. da Cunha, N. B.; Cobacho, N. B.; Viana, J. F.; Lima, L. A.; Sampaio, K. B.; Dohms, S. S.; Ferreira, A. C.; la Fuente-Núñez, C.; Costa, F. F.; Franco, O. L.; Dias, S. C. The Next Generation of Antimicrobial Peptides (Amps) as Molecular Therapeutic Tools for the Treatment of Diseases with Social and Economic Impacts. *Drug Discov. Today.* **2017,** 22, 234-248.

(7) Ageitos, J. M.; Sánchez-Pérez, A.; P.Calo-Mata; T.G.Villa. Antimicrobial Peptides (Amps): Ancient Compounds That Represent Novel Weapons in the Fight against Bacteria. *Biochem. Pharmacol.* **2017,** 133, 117-138.

(8) Kang, H. K.; Kim, C.; Seo, C. H.; Park, Y. The Therapeutic Applications of Antimicrobial Peptides (Amps): A Patent Review. *J. Microbiol.* **2017,** 55, 1-12.

(9) Yeaman, M. R.; Yount, N. Y. Mechanisms of Antimicrobial Peptide Action and Resistance. *Pharmacol. Rev.* **2003,** 55, 27-55.

(10) Melo, M. N.; Ferre, R.; Castanho, M. A. Antimicrobial Peptides: Linking Partition, Activity and High Membrane-Bound Concentrations. *Nat. Rev. Microbiol.* **2009,** 7, 245-250.

(11) Brogden, K. A. Antimicrobial Peptides: Pore Formers or Metabolic Inhibitors in Bacteria? *Nat. Rev. Microbiol.* **2005,** 3, 238-250.

(12) Perron, G. G.; Zasloff, M.; Bell, G. Experimental Evolution of Resistance to an Antimicrobial Peptide. *Proc. Biol. Sci.* **2006,** 273, 251-256.

(13) Peschel, A.; Sahl, H. G. The Co-Evolution of Host Cationic Antimicrobial Peptides and Microbial Resistance. *Nat. Rev. Microbiol.* **2006,** 4, 529-536.

(14) Fjell, C. D.; Hiss, J. A.; Hancock, R. E.; Schneider, G. Designing Antimicrobial Peptides: Form Follows Function. *Nat. Rev. Drug Discov.* **2012,** 11, 37-51.

(15) Tew, G. N.; Scott, R. W.; Klein, M. L.; Degrado, W. F. De Novo Design of Antimicrobial Polymers, Foldamers, and Small Molecules: From Discovery to Practical Applications. *Acc. Chem. Res.* **2010,** 43, 30-39.

(16) Hamuro, Y.; Schneider, J. P.; DeGrado, W. F. De Novo Design of Antibacterial B-Peptides. *J. Am. Chem. Soc.* **1999,** 121, 12200-12201.

(17) Liu, D.; DeGrado, W. F. De Novo Design, Synthesis, and Characterization of Antimicrobial Beta-Peptides. *J. Am. Chem. Soc.* **2001,** 123, 7553-7559.

(18) Porter, E. A.; Wang, X.; Lee, H. S.; Weisblum, B.; Gellman, S. H. Non-Haemolytic Beta-Amino-Acid Oligomers. *Nature* **2000,** 404, 565.

(19) Raguse, T. L.; Porter, E. A.; Weisblum, B.; Gellman, S. H. Structure-Activity Studies of 14-Helical Antimicrobial Beta-Peptides: Probing the Relationship between Conformational Stability and Antimicrobial Potency. *J. Am. Chem. Soc.* **2002,** 124, 12774-12785.

(20) Porter, E. A.; Weisblum, B.; Gellman, S. H. Mimicry of Host-Defense Peptides by Unnatural Oligomers: Antimicrobial Beta-Peptides. *J. Am. Chem. Soc.* **2002,** 124, 7324-7330.

(21) Arvidsson, P. I.; Ryder, N. S.; Weiss, H. M.; Hook, D. F.; Escalante, J.; Seebach, D. Exploring the Antibacterial and Hemolytic Activity of Shorter- and Longer-Chain Beta-, Alpha,Beta-, and Gamma-Peptides, and of Beta-Peptides from Beta2-3-Aza- and Beta3-2-Methylidene-Amino Acids Bearing Proteinogenic Side Chains--a Survey. *Chem. Biodivers.* **2005,** 2, 401-420.

(22) Marr, A. K.; Gooderham, W. J.; Hancock, R. E. Antibacterial Peptides for Therapeutic Use: Obstacles and Realistic Outlook. *Curr. Opin. Pharmacol.* **2006,** 6, 468-472.

(23) Vaara, M. New Approaches in Peptide Antibiotics. *Curr. Opin. Pharmacol.* **2009,** 9, 571-576.

(24) Patch, J. A.; Barron, A. E. Helical Peptoid Mimics of Magainin-2 Amide. *J. Am. Chem. Soc.* **2003,** 125, 12092-12093.

(25) Violette, A.; Fournel, S.; Lamour, K.; Chaloin, O.; Frisch, B.; Briand, J. P.; Monteil, H.; Guichard, G. Mimicking Helical Antibacterial Peptides with Nonpeptidic Folding Oligomers. *Chem. Biol.* **2006,** 13, 531-538.

(26) Claudon, P.; Violette, A.; Lamour, K.; Decossas, M.; Fournel, S.; Heurtault, B.; Godet, J.; Mely, Y.; Jamart-Gregoire, B.; Averlant-Petit, M. C.; Briand, J. P.; Duportail, G.; Monteil, H.; Guichard, G. Consequences of Isostructural Main-Chain Modifications for the Design of Antimicrobial Foldamers: Helical Mimics of Host-Defense Peptides Based on a Heterogeneous Amide/Urea Backbone. *Angew. Chem. Int. Ed. Engl.* **2010,** 49, 333-336.

(27) Tew, G. N.; Liu, D.; Chen, B.; Doerksen, R. J.; Kaplan, J.; Carroll, P. J.; Klein, M. L.; DeGrado, W. F. De Novo Design of Biomimetic Antimicrobial Polymers. *Proc. Natl. Acad. Sci.* **2002,** 99, 5110-5114.

(28) Liu, D.; Choi, S.; Chen, B.; Doerksen, R. J.; Clements, D. J.; Winkler, J. D.; Klein, M. L.; DeGrado, W. F. Nontoxic Membrane-Active Antimicrobial Arylamide Oligomers. *Angew. Chem. Int. Ed. Engl.* **2004,** 43, 1158-1162.

(29) Choi, S.; Isaacs, A.; Clements, D.; Liu, D.; Kim, H.; Scott, R. W.; Winkler, J. D.; DeGrado, W. F. De Novo Design and in Vivo Activity of Conformationally Restrained Antimicrobial Arylamide Foldamers. *Proc. Natl. Acad. Sci.* **2009,** 106, 6968-6973.

(30) Hua, J.; Yamarthy, R.; Felsenstein, S.; Scott, R. W.; Markowitz, K.; Diamond, G. Activity of Antimicrobial Peptide Mimetics in the Oral Cavity: I.

Activity against Biofilms of Candida Albicans. *Mol. Oral Microbiol.* **2010,** 25, 418-425.

(31) Hua, J.; Scott, R. W.; Diamond, G. Activity of Antimicrobial Peptide Mimetics in the Oral Cavity: Ii. Activity against Periopathogenic Biofilms and Anti-Inflammatory Activity. *Mol. Oral Microbiol.* **2010,** 25, 426-432.

(32) Tang, H.; Doerksen, R. J.; Tew, G. N. Synthesis of Urea Oligomers and Their Antibacterial Activity. *Chem. Commun.* **2005**, 1537-1539.

(33) Arnt, L.; Nüsslein, K.; Tew, G. N. Nonhemolytic Abiogenic Polymers as Antimicrobial Peptide Mimics. *J. Polym. Scie. Part A: Polym. Chem.* **2004,** 42, 3860-3864.

(34) *ClinicalTrials NCT020388*.

(35) Mathieu, L.; Legrand, B.; Deng, C.; Vezenkov, L.; Wenger, E.; Didierjean, C.; Amblard, M.; Averlant-Petit, M. C.; Masurier, N.; Lisowski, V.; Martinez, J.; Maillard, L. T. Helical Oligomers of Thiazole-Based Gamma-Amino Acids: Synthesis and Structural Studies. *Angew. Chem. Int. Ed. Engl.* **2013,** 52, 6006-6010.

(36) Legrand, B.; Mathieu, L.; Lebrun, A.; Andriamanarivo, S.; Lisowski, V.; Masurier, N.; Zirah, S.; Kang, Y. K.; Martinez, J.; Maillard, L. T. Thiazole-Based Gamma-Building Blocks as Reverse-Turn Mimetic to Design a Gramicidin S

Analogue: Conformational and Biological Evaluation. *Chem. Eur. J.* **2014,** 20, 6713-6720.

(37) Bonnel, C.; Legrand, B.; Bantignies, J. L.; Petitjean, H.; Martinez, J.; Masurier, N.; Maillard, L. T. Ft-Ir and Nmr Structural Markers for Thiazole-Based Gamma-Peptide Foldamers. *Org. Biomol. Chem.* **2016,** 14, 8664-8669.

(38) Bonnel, C.; Legrand, B.; Simon, M.; Martinez, J.; Bantignies, J. L.; Kang, Y. K.; Wenger, E.; Hoh, F.; Masurier, N.; Maillard, L. T. C9/12 Ribbon-Like Structures in Hybrid Peptides Alternating Alpha- and Thiazole-Based Gamma-Amino Acids. *Chem. Eur. J.* **2017,** 23, 17584-17591.

(39) Aguesseau-Kondrotas, J.; Simon, M.; Legrand, B.; Bantignies, J. L.; Kang, Y. K.; Dumitrescu, D.; Van Der Lee, A.; Campagne, J. M.; de Figueiredo, R. M.; Maillard, L. T. Prospect of Thiazole-Based Gamma-Peptide Foldamers in Enamine Catalysis: Exploration of the Nitro-Michael Addition. *Chem. Eur. J.* **2019,** 25, 7396-7401.

(40) Simon, M.; Ali, L. M. A.; Cheikh, K. E.; Aguesseau, J.; Gary-Bobo, M.; Garcia, M.; Morère, A.; Maillard, L. T. Can Heterocyclic Γ-Peptides Provide Polyfunctional Platforms for Synthetic Glycocluster Construction? *Chem. Eur. J.* **2018,** 24, 11426-11432.

(41) Ali, L. M. A.; Simon, M.; El Cheikh, K.; Aguesseau-Kondrotas, J.; Godefroy, A.; Nguyen, C.; Garcia, M.; Morere, A.; Gary-Bobo, M.; Maillard, L. Topological Requirements for Ci-M6pr-Mediated Cell Uptake. *Bioconjugate Chem.* **2019,** 30, 2533-2538.

(42) Mathieu, L.; Bonnel, C.; Masurier, N.; Maillard, L. T.; Martinez, J.; Lisowski, V. Cross-Claisen Condensation of N-Fmoc-Amino Acids – a Short Route to Heterocyclic Γ-Amino Acids. *Eur. J. Org. Chem.* **2015,** 2015, 2262-2270.

(43) Case, D. A.; Betz, R. M.; Cerutti, D. S.; T.E. Cheatham, I.; Darden, T. A.; Duke, R. E.; Giese, T. J.; Gohlke, H.; Goetz, A. W.; Homeyer, N.; Izadi, S.; Janowski, P.; Kaus, J.; Kovalenko, A.; Lee, T. S.; LeGrand, S.; Li, P.; Lin, C.; Luchko, T.; Luo, R.; Madej, B.; Mermelstein, D.; Merz, K. M.; Monard, G.; Nguyen, H.; Nguyen, H. T.; Omelyan, I.; Onufriev, A.; Roe, D. R.; Roitberg, A.; Sagui, C.; Simmerling, C. L.; Botello-Smith, W. M.; Swails, J.; Walker, R. C.; Wang, J.; Wolf, R. M.; Wu, X.; Xiao, L.; Kollman, P. A. *Amber 16*, University of California, San Francisco, 2016.

(44) Frisch, M. J.; Trucks, G. W.; Schlegel, H. B.; Scuseria, G. E.; Robb, M. A.; Cheeseman, J. R.; Scalmani, G.; Barone, V.; Mennucci, B.; Petersson, G. A.; Nakatsuji, H.; Caricato, M.; Li, X.; Hratchian, H. P.; Izmaylov, A. F.; Bloino, J.;

Zheng, G.; Sonnenberg, J. L.; Hada, M.; Ehara, M.; Toyota, K.; Fukuda, R.; Hasegawa, J.; Ishida, M.; Nakajima, T.; Honda, Y.; Kitao, O.; Nakai, H.; Vreven, T.; Montgomery Jr., J. A.; Peralta, J. E.; Ogliaro, F.; Bearpark, M. J.; Heyd, J.; Brothers, E. N.; Kudin, K. N.; Staroverov, V. N.; Kobayashi, R.; Normand, J.; Raghavachari, K.; Rendell, A. P.; Burant, J. C.; Iyengar, S. S.; Tomasi, J.; Cossi, M.; Rega, N.; Millam, N. J.; Klene, M.; Knox, J. E.; Cross, J. B.; Bakken, V.; Adamo, C.; Jaramillo, J.; Gomperts, R.; Stratmann, R. E.; Yazyev, O.; Austin, A. J.; Cammi, R.; Pomelli, C.; Ochterski, J. W.; Martin, R. L.; Morokuma, K.; Zakrzewski, V. G.; Voth, G. A.; Salvador, P.; Dannenberg, J. J.; Dapprich, S.; Daniels, A. D.; Farkas, Ö.; Foresman, J. B.; Ortiz, J. V.; Cioslowski, J.; Fox, D. J. *Gaussian 09 - Wallingford, Ct, USA - Gaussian, Inc.*, Gaussian, Inc.: Wallingford, CT, USA, 2009.

(45) Yang, L.; Harroun, T. A.; Weiss, T. M.; Ding, L.; Huang, H. W. Barrel-Stave Model or Toroidal Model? A Case Study on Melittin Pores. *Biophys. J.* **2001,** 81, 1475-1485.

(46) Rakowska, P. D.; Jiang, H.; Ray, S.; Pyne, A.; Lamarre, B.; Carr, M.; Judge, P. J.; Ravi, J.; Gerling, U. I.; Koksch, B.; Martyna, G. J.; Hoogenboom, B. W.; Watts, A.; Crain, J.; Grovenor, C. R.; Ryadnov, M. G. Nanoscale Imaging Reveals

Laterally Expanding Antimicrobial Pores in Lipid Bilayers. *Proc. Natl. Acad. Sci.* **2013,** 110, 8918-8923.

(47) Zhang, S. K.; Song, J. W.; Gong, F.; Li, S. B.; Chang, H. Y.; Xie, H. M.; Gao, H. W.; Tan, Y. X.; Ji, S. P. Design of an Alpha-Helical Antimicrobial Peptide with Improved Cell-Selective and Potent Anti-Biofilm Activity. *Sci. Rep.* **2016,** 6, 1-13.

(48) Juba, M. L.; Porter, D. K.; Williams, E. H.; Rodriguez, C. A.; Barksdale, S. M.; Bishop, B. M. Helical Cationic Antimicrobial Peptide Length and Its Impact on Membrane Disruption. *Biochim. Biophys. Acta* **2015,** 1848, 1081-1091.

(49) Hartmann, M.; Berditsch, M.; Hawecker, J.; Ardakani, M. F.; Gerthsen, D.; Ulrich, A. S. Damage of the Bacterial Cell Envelope by Antimicrobial Peptides Gramicidin S and Pgla as Revealed by Transmission and Scanning Electron Microscopy. *Antimicrob. Agents Chemother.* **2010,** 54, 3132-3142.

(50) Duval, E.; Zatylny, C.; Laurencin, M.; Baudy-Floc'h, M.; Henry, J. Kkkkplfglffglf: A Cationic Peptide Designed to Exert Antibacterial Activity. *Peptides* **2009,** 30, 1608-1612.

(51) Sims, P. J.; Waggoner, A. S.; Wang, C.-H.; Hoffman, J. F. Mechanism by Which Cyanine Dyes Measure Membrane Potential in Red Blood Cells and Phosphatidylcholine Vesicles. *Biochemistry* **1974,** 13, 3315–3330.

(52) Te Winkel, J. D.; Gray, D. A.; Seistrup, K. H.; Hamoen, L. W.; Strahl, H. Analysis of Antimicrobial-Triggered Membrane Depolarization Using Voltage Sensitive Dyes. *Front. Cell. Dev. Biol.* **2016,** 4, Article 29, 21-10.

(53) Cabrini, G.; Verkman, A. S. Potential-Sensitive Response Mechanism of Dis-C3-(5) in Biological Membranes. *J. Membr. Biol.* **1986,** 92, 171-182.

(54) Johnson, B. A.; Blevins, R. A. Nmr View: A Computer Program for the Visualization and Analysis of Nmr Data. *J. Biomol. NMR* **1994,** 4, 603-614.

(55) Wüthrich, K. *Nmr of Proteins and Nucleic Acids*. John Wiley & Sons, Inc.: New-York, 1986.

(56) Koradi, R.; Billeter, M.; Wuthrich, K. Molmol: A Program for Display and Analysis of Macromolecular Structures. *J. Mol. Graph. 1996, 14, 51.* **1996,** 14, 51-55.

(57) Pettersen, E. F.; Goddard, T. D.; Huang, C. C.; Couch, G. S.; Greenblatt, D. M.; Meng, E. C.; Ferrin, T. E. Ucsf Chimera--a Visualization System for Exploratory Research and Analysis. *J. Comput. Chem.* **2004,** 25, 1605-1612.

(58) Zhao, Y.; Truhlar, D. G. The M06 Suite of Density Functionals for Main Group Thermochemistry, Thermochemical Kinetics, Noncovalent Interactions, Excited States, and Transition Elements: Two New Functionals and Systematic

Testing of Four M06-Class Functionals and 12 Other Functionals. *Theor. Chem. Acc.* **2008,** 120, 215.

(59) Marenich, A. V. C., C. J.; Truhlar, D. G. J. . Universal Solvation Model Based on Solute Electron Density and on a Continuum Model of the Solvent Defined by the Bulk Dielectric Constant and Atomic Surface Tensions. *Phys. Chem. B* . **2009,** 113, 6378.

(60) Singh, U. C.; Kollman, P. A. An Approach to Computing Electrostatic Charges for Molecules. *J. Comput. Chem.* **1984,** 5, 129-145.

(61) Besler, B. H.; Merz, K. M.; Kollman, P. A. Atomic Charges Derived from Semiempirical Methods. *J. Comput. Chem.* **1990,** 11, 431-439.

(62) Kim, M. K.; Kang, N.; Ko, S. J.; Park, J.; Park, E.; Shin, D. W.; Kim, S. H.; Lee, S. A.; Lee, J. I.; Lee, S. H.; Ha, E. G.; Jeon, S. H.; Park, Y. Antibacterial and Antibiofilm Activity and Mode of Action of Magainin 2 against Drug-Resistant Acinetobacter Baumannii. *Int. J. Mol. Sci.* **2018,** 19, 3041.

Authors are required to submit a graphic entry for the Table of Contents (TOC) that, in conjunction with the manuscript title, should give the reader a representative idea of one of the following: A key structure, reaction, equation, concept, or theorem, etc., that is discussed in the manuscript. Consult the journal's Instructions for Authors for TOC graphic specifications.